iScience

Article

Metabolomics and metagenomics in mice reveal the role of the gut microbiota in tryptophan metabolism

Graphical abstract

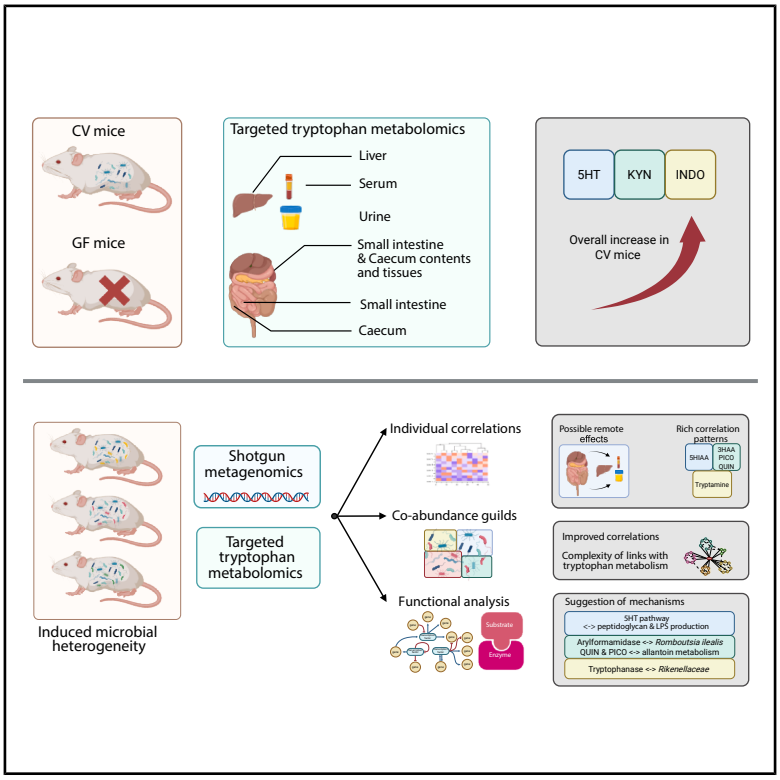

Highlights

- Tryptophan metabolism is extensively altered in germ-free mice
- Some bacterial co-abundance guilds are potential actors of tryptophan metabolism
- Functional analysis highlights potential mechanisms of the host-microbiota dialog

Authors

Margaux Levé, Paolo Manghi, Marius Bredon, ..., Nathalie Rolhion, Nicola Segata, Harry Sokol

Correspondence

harry.sokol@gmail.com

In brief

Metabolomics; Microbiome

Levé et al., 2025, iScience *28*, 113751
November 21, 2025
https://doi.org/10.1016/j.isci.2025.113751

CellPress

iScience

CellPress
OPEN ACCESS

Article

Metabolomics and metagenomics in mice reveal the role of the gut microbiota in tryptophan metabolism

Margaux Levé,[1,2] Paolo Manghi,[3] Marius Bredon,[1,2] Antoine Lefevre,[4] Serena Manara,[3] Federica Armanini,[3] Patrick Emond,[4,7] Julien Planchais,[2,5] Nathalie Rolhion,[1,2] Nicola Segata,[3,6] and Harry Sokol[1,2,5,8,*]

[1]Sorbonne Université, INSERM, Centre de Recherche Saint-Antoine, CRSA, AP-HP, Saint-Antoine Hospital, Gastroenterology Department, 75012 Paris, France
[2]Gut, Liver & Microbiome Research (GLIMMER) FHU, Paris, France
[3]Department CIBIO, University of Trento, Trento, Italy
[4]UMR 1253, iBrain, University of Tours, Inserm, Tours, France
[5]Université Paris-Saclay, INRAe, AgroParisTech, Micalis institute, Jouy-en-Josas, France
[6]IEO, European Institute of Oncology IRCCS, Milan, Italy
[7]CHRU de Tours, service de médecine nucléaire in vitro, Tours, France
[8]Lead contact
*Correspondence: harry.sokol@gmail.com
https://doi.org/10.1016/j.isci.2025.113751

SUMMARY

Tryptophan metabolism plays a key role in host-microbiota interactions, producing a wide array of bioactive metabolites. However, our understanding of the interactions between tryptophan metabolites and the gut microbiota is still limited. Using targeted quantitative metabolomics and metagenomics in mice across various compartments, we showed that the cecal microbiota massively impacts tryptophan metabolism both in the gut and systemically. Grouping bacterial taxa in co-abundance guilds better reflected the links between gut microbes and tryptophan metabolites than single taxa taken individually and suggested the involvement of complex microbial interactions in tryptophan metabolism regulation. Finally, analyzing functional data, we shed light on the potential links between tryptophan metabolism and bacterial enzymes or metabolic pathways.

INTRODUCTION

The gut microbiota is a complex ecosystem living in symbiosis with humans in the gastrointestinal tract. It is essential to human health for functions such as immune maturation and regulation,[1,2] protection against pathogens,[3] digestion, and absorption of nutrients.[4] Its disturbance is associated with a growing number of diseases. The host-microbiota interactions rely on multiple mechanisms, including the production and degradation of metabolites by either microorganisms from the gut lumen or host cells. Then, metabolites can either contribute to host cells' metabolism locally or act systemically by crossing the intestinal barrier and reaching the general blood circulation after passing the portal circulation and the liver. We and others have recently shown the importance of tryptophan (Trp) metabolism in host-microbiome interactions and human health. Indeed, it has been found to be disturbed in diseases like irritable bowel diseases, inflammatory bowel diseases,[5] neuropsychiatric disorders,[6] obesity and metabolic syndrome,[7] or celiac disease.[8] Trp can be transformed into other metabolites through three main pathways: serotonin, kynurenine (Kyn), and indole pathways. The gut microbiota can influence the first two pathways and directly acts in the third one.[6]

Serotonin (5HT, 5-hydroxytryptamine) production mainly occurs in the host's enterochromaffin cells. Indeed, before being further metabolized into 5HT and released in the blood circulation, 5-OH-tryptophan (5HTP) is produced into enterochromaffin cells from Trp through the action of Trp hydroxylase 1 (Tph1) enzyme.[6] 5HT is one of the most important neurotransmitters for intestine functioning, as it is involved in peristalsis, motility, and secretion signaling.[9] Its main degradation product is 5-OH-indole acetic acid (5HIAA), but it can also be transformed into melatonin, another important neuro-hormone. The gut microbiota, especially spore-forming bacteria, can influence 5HT production in the colon by regulating Tph1 levels,[10] but the mechanisms are still poorly understood.

The initial and limiting step of the Kyn pathway is the transformation of Trp into Kyn. It occurs in many cell types, including immune and epithelial cells, and is mediated in the gut by the IDO1 enzyme. The Kyn pathway shows four main end products that are particularly involved in neurotransmission, inflammation, and immune response: picolinic acid (PICO), quinolinic acid (QUIN), kynurenic acid (KYNA), and xanthurenic acid (XANA). The Kyn pathway is greatly disturbed in germ-free mice,[11] and IDO1 activity is believed to be indirectly influenced by the gut microbiota through the stimulation of cytokine production by

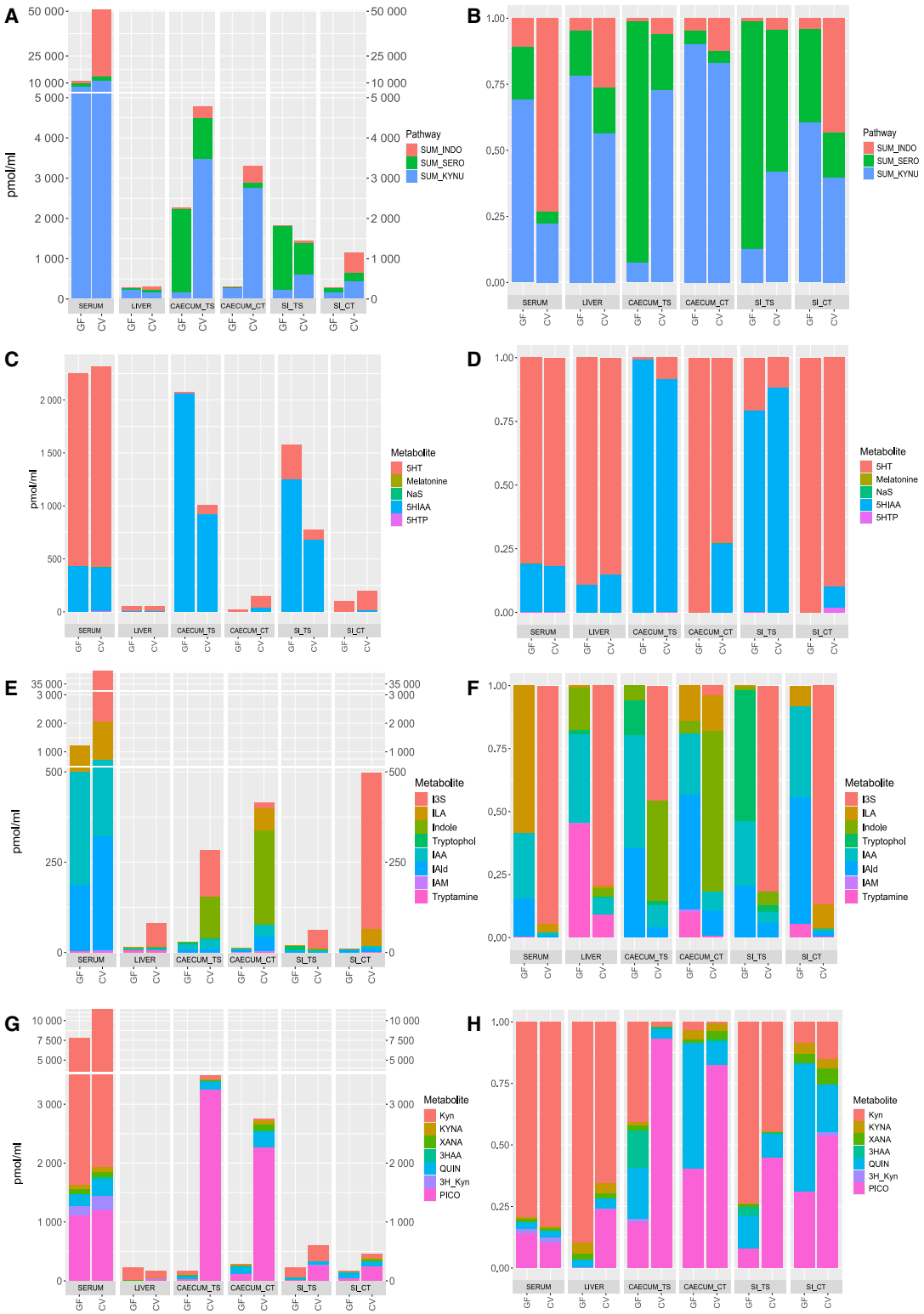

Figure 1. The gut microbiota plays a major role in tryptophan metabolism

Comparison of concentrations of Trp metabolites between GF and CV mice. Concentrations are in pmol/mL.

(A) Cumulative absolute concentrations by pathways. Concentrations were summed over each pathway (indoles, serotonin, kynurenine) and then averaged over all GF or CV mice.

(legend continued on next page)

immune cells.[12] To a limited extent, bacteria like members of the *Romboutsia* genus can directly produce Kyn from Trp by expressing arylformamidase.[13] Thus, microbial interactions with the Kyn pathway are complex and there is still a lot to discover.

Finally, Trp transformation into metabolites of the indole pathway is directly due to microbial activity. Many indole derivatives are ligands for the aryl hydrocarbon receptor (AhR) expressed by both intestinal and immune cells, whose signaling has many functions for the host, including maintenance of barrier integrity, immunity, or epithelial renewal.[14] These metabolites are also involved in bacterial interspecies interactions, making them key regulators of both the host-microbiota system and the microbial community. A growing number of bacterial species are being identified as AhR ligand producers, such as *Lactobacillus* spp.,[5] members of the *Clostridium* genus,[15] or bacteria expressing tryptophanase, an enzyme allowing for Trp transformation into indole, like *Escherichia coli* or *Bacteroides thetaiotaomicron*.[14,16] Many of these bacteria are commensals of the gut microbiota. Although there have been many findings regarding the importance of this pathway recently, many microbial actors are still to be discovered, as well as the mechanisms underlying their effects.

Interestingly, these three pathways are not independent. Some metabolites of the Kyn pathway can act as AhR ligands, like Kyn, KYNA, and XANA. 5HIAA was also found to be an AhR ligand in B cells,[17] and 5HT can indirectly stimulate AhR activity by inhibiting AhR ligand processing by CYP1A1.[18] In addition, Trp metabolites dynamically evolve in the host organism, with movements between the gut lumen, intestinal tissues, and systemic circulation that are still poorly understood. Thus, very complex mechanisms and interactions underlie Trp metabolism, encouraging further research about it.

In this study, we explored the link between Trp metabolism and the gut microbiome, aiming at identifying new microbial actors or functions that could participate in Trp metabolism. For this, we first compared Trp metabolite levels in various types of biological samples between germ-free (GF) and conventionalized (CV) mice, confirming the essential role of the gut microbiota in Trp metabolism. Then, analyzing metabolomics and shotgun metagenomics data from 50 other mice with high microbiome heterogeneity as a result of various diet or antibiotic treatments, we showed that the cecal microbiota had a preponderant role over the ileal microbiota regarding Trp metabolism. Also, we showed that the cecal microbiota could influence Trp metabolism both locally and at a systemic level. The individual correlation patterns highlighted new potential actors but remained very complex, so we grouped microbial species into co-abundance guilds, improving the strength of microbiome-Trp metabolite correlations and identifying groups of microbes that could be particularly linked to Trp metabolism. This analysis also suggested that Trp metabolism regulation relies on more sophisticated microbial interactions. Finally, analyzing functional data including Enzyme Commission (EC) enzymes and MetaCyc pathways abundances, we highlighted interesting potential links between bacterial functions and Trp metabolites.

RESULTS

The gut microbiota plays a major role in tryptophan metabolism

To investigate the role of the gut microbiota in Trp metabolism, we compared the levels of Trp metabolites between GF and CV mice. Using targeted quantitative metabolomics, metabolites of the three pathways (serotonin, Kyn, and indole) were measured in the following different compartments: the ileum tissue, the small intestine (SI) content, the cecum tissue, the cecum content, the liver, and the serum.

Substantial differences were found between GF and CV mice in the three Trp metabolism pathways, as shown by summing the concentrations of the metabolites by pathways (Figures 1A and 1B), suggesting that the gut microbiota has a major effect on Trp metabolism.

Transformation of Trp into 5HT and other related metabolites is mainly due to the activity of host's enterochromaffin cells, but it has been found that the gut microbiota can also impact this metabolic pathway.[10] Here, we found that the serotonin pathway was disturbed in GF mice, especially in intestinal compartments, thus indirectly confirming the contribution of the gut microbiota in its regulation (Figures 1C, 1D, and S1). The most remarkable differences between CV and GF mice involved the levels of 5HT and 5HIAA. Indeed, in GF mice, the concentration of 5HT was significantly decreased in the cecum tissue, cecum content, and SI content. However, 5HT levels in the serum did not differ between GF and CV mice. 5HIAA was significantly increased in the cecum and ileum tissues and decreased in the cecum and SI contents of GF mice, suggesting that the gut microbiota activity can also influence the production of this metabolite. Interestingly, the levels of 5HTP, the precursor of 5HT, were significantly reduced in the serum and the SI content of GF mice. This suggests that 5HTP production could be stimulated by microbial activity especially in the SI compared to the cecum and that this stimulation could impact 5HTP blood levels.

The indole metabolites, which are almost exclusively produced by the gut microbiota, were indeed extremely reduced in all compartments in GF compared to CV mice, in terms of absolute concentration and of proportion of Trp metabolism. Figures 1E and 1F show that the strongest effect was seen for indole-3-sulfate (I3S), which is not produced at all in GF mice. Of note, serum I3S levels in our study were all above 20,000 pmol/mL. In other studies, those levels are substantially variable in healthy mice, ranging from about 2,000 to 63,000 pmol/mL.[19–25] Serum levels of I3S are known to be

(B) Cumulative relative concentrations by pathway. Concentrations were summed over each pathway (indoles, serotonin, kynurenine), averaged over all GF or CV mice, and then normalized by the sum of the three pathways. INDO: indole pathway, SERO: serotonin pathway, KYNU: kynurenine pathway.
(C and D) Absolute concentrations (C) and relative concentration (D) of metabolites from the serotonin pathway averaged over all GF or CV mice.
(E and F) Absolute concentrations (E) and relative concentration (F) of metabolites from the indole pathway averaged over all GF or CV mice.
(G and H) Absolute concentrations (G) and relative concentration (H) of metabolites from the kynurenine pathway averaged over all GF or CV mice.

increased in case of impaired renal function.[20,25] However, one study compared serum levels of I3S between healthy male and female mice and found a significant difference between the two genders (63,340 pmol/mL for females and 17,480 pmol/mL for males).[25] Hence, it is possible that our results reflect gender differences as we only used female mice. I3S is a good example of host-microbiota co-metabolism. Some members of the gut microbiota produce indole from the metabolism of Trp. Indole is then absorbed and reaches the liver through the portal circulation, where it is metabolized by a mammalian enzyme to form I3S.[26] In agreement with this metabolic sequence, indole was significantly decreased in the cecum tissue and cecum content of GF mice, and I3S was only found in the liver and serum of CV mice. Similarly, indole-3-lactic acid (ILA) and other indole derivatives such as indole-3-acetic acid (IAA), indole-3-aldehyde (IAld), and tryptamine are significantly decreased in the cecum content of GF mice, demonstrating a strong microbial activity in this compartment regarding the indole pathway (Figure S2). Surprisingly, serum ILA and IAld levels were significantly decreased in GF mice but were non-zero and serum IAA levels were similar in GF and CV mice. In comparison, indole and I3S were absent in the serum of GF mice. Other studies found similar results with the detection of IAA, IAld, and ILA in the serum of GF mice[27,28] and undetected levels of indole and I3S.[21] These results suggest an endogenous production of IAA, IAld, and ILA in addition to microbial production, while indole and its liver derivative I3S strictly depend on microbial activity. In line with this hypothesis, it was found that human and mice immune cells could transform Trp into IPA, the precursor of IAA, IAld, and ILA, via IL4I1 expression.[29–31] It is also possible that diet influences the levels of IAA and ILA, as these compounds are known plant auxins (growth hormones).[32–34]

Finally, the Kyn pathway was also importantly impacted by the gut microbiota (Figures 1G, 1H, and S3). While the total production of metabolites from this pathway was increased in the liver of GF mice, it was decreased in all other compartments except the cecum. Kyn metabolites followed the same pattern, suggesting that the gut microbiota directly or indirectly regulates the transformation of Trp into Kyn. This is in agreement with the fact that the activity of IDO1, the enzyme metabolizing Trp into Kyn in the gut, was found to be stimulated by the gut microbiota.[6] However, it is also likely that the microbiota stimulates the recruitment of immune cells harboring high IDO1 activity in the gut and thus indirectly contributes to the induction of this pathway in the gastrointestinal tract.[12] In addition, all metabolites of the Kyn pathway except 3-OH-kynurenine (3H-kyn) were significantly reduced in the cecum content and all final products of this pathway (KYNA, XANA, QUIN, and PICO) were further significantly decreased in the cecum tissue of GF mice, demonstrating the influence of microbial activity in this pathway. The effects of microbiota depletion on these final products were also strong in the SI (Figure S3).

All these results show that the three Trp metabolism pathways are highly impacted by the gut microbiota activity, particularly in intestinal compartments. Figure 2 summarizes the significant changes between GF and CV mice.

The cecal microbiota shows complex correlations with tryptophan metabolites, especially in the cecum content and the serum

To better understand how microbial populations and Trp metabolism are linked, we designed a specific experiment in which we correlated Trp metabolism and gut microbiome composition (Figure 3A). In order to induce a high microbiome and metabolome heterogeneity and thus increase the statistical power to find relevant correlations between them, 50 mice submitted to different microbiota perturbations were included. More precisely, mice were either fed with a low- or high-Trp diet, fed with a high-milk-fat diet or high-fat diet, or received different antibiotic treatments (vancomycin, penicillin, ofloxacin, metronidazole, or colistin). The other mice were bred as controls. Trp metabolites were analyzed using the same approach as above, and the gut microbiome was analyzed in both the cecum and SI compartments using shotgun metagenomics. Bacterial species were retrieved using the species-level genome bin (SGB) system.

We observed significant false discovery rate (FDR)-adjusted correlations between Trp metabolites and members of the cecum microbiota, but not with the SI ones (Figure 3B). This suggests a more preponderant role of the cecum microbiota in the regulation of Trp metabolism, in agreement with its greater biomass and richness compared to the SI. As expected, among the different compartments, the cecum microbiota showed the strongest correlations with metabolites from the cecum content. Interestingly, it also correlated substantially with metabolites from the serum, suggesting that the cecal microbiota could have a remote influence at a systemic level.

Taken together, and in light of the above-described analysis in germ-free mice, these results suggest that the cecum microbiota impacts the Trp metabolism not only locally, in the cecum content but also at regional and systemic levels. Importantly, only a limited number of metabolites, all belonging to the Kyn and indole pathways, were significantly correlated with only one SGB: cecum tissue Trp (SGB41677), cecum content PICO (SGB43540), SI tissue PICO (SGB43530), cecum tissue QUIN (SGB59899), serum 3H-kyn (SGB42491), SI content XANA (SGB41545), serum IAA, SI content IAld and cecum content IAld with SGB41594, SI tissue tryptophol (SGB33556), and urine IAA (SGB33580, *Atopobiaceae bacterium* FL090493). This further raises the idea that complex microbial interactions could be involved in Trp metabolism.

When considering the serotonin pathway (Figure 3C), the strongest correlations with the cecal microbiota were observed with serum 5HT. This confirms that microbial populations in the gut may influence systemic 5HT level. Interestingly, cecal microbiota also correlated with the SI level of 5HTP, which is the direct precursor of 5HT, suggesting also an effect of the cecal microbiota on 5HT production in the SI. Moreover, no correlations were found with 5HTP in systemic compartments (except urine) supporting that 5HTP is mostly transformed into 5HT locally, in agreement with other findings showing that the gut microbiota could promote Tph1 expression into enterochromaffin cells.[10] Interestingly, the level of 5HIAA and N-acetyl-serotonin (NaS), the two 5HT degradation products, in different gastrointestinal compartments but not in serum, showed strong correlations with the cecal microbiota,

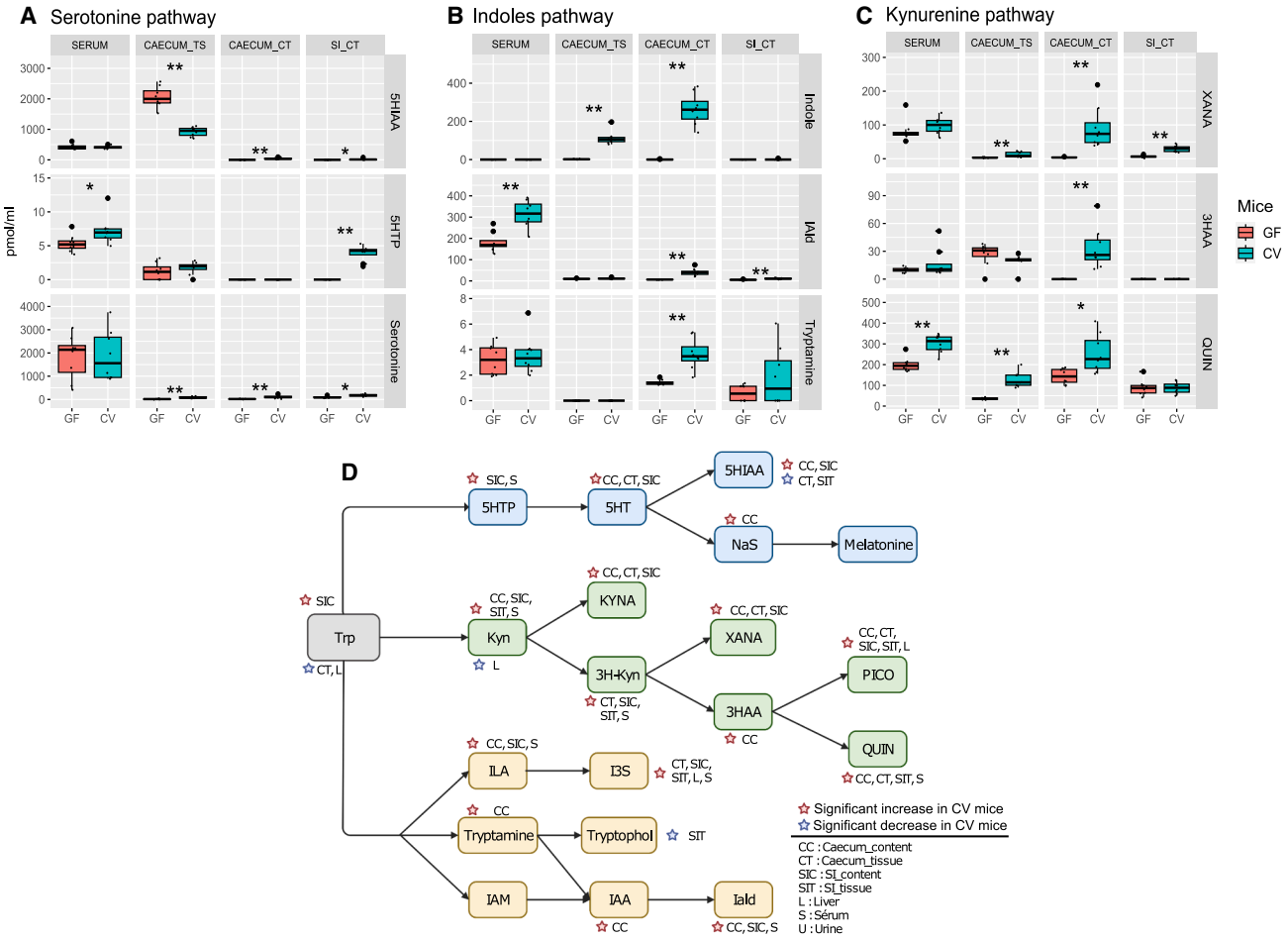

Figure 2. Significant changes in Trp metabolites between GF and CV mice

(A–C) Boxplots showing the concentrations of a selection of serotonin (A), indole (B), and kynurenine (C) pathway metabolites. Metabolite level medians between GF and CV mice were statistically compared using non-parametric Wilcoxon test (Mann-Whitney test), and *p* values were adjusted using the Benjamini-Hochberg procedure: **p* adjusted <0.05, ***p* adjusted <0.01. Results for all metabolites are shown in Figures S1–S3.

(D) Summary of changes in metabolites concentrations between GF and CV mice. Red stars: significant increase of the metabolite in CV mice, blue stars: significant decrease of the metabolite in CV mice. Changes were considered significant if *p* adjusted <0.05.

suggesting that the gut microbiota could influence local 5HT degradation in the gut. SGBs showing positive correlations with both cecum content 5HIAA and NaS were numerous and were mostly Bacillota (formerly Firmicutes) from the Lachnospiraceae and Ruminococcaceae families, as well as Actinomycetes (formerly Actinobacteria) from the Nocardiaceae family. This suggests that these SGBs could be involved in the degradation of 5HT locally in the gut after its release by enterochromaffin cells. Some of these SGBs were also positively correlated to SI tissue 5HTP, which further suggests that they may be able to promote 5HT production by inducing Tph1 expression. These SGBs were all unknown species (Nocardiaceae: SGB43264 and SGB43267; unclassified bacteria: SGB41598; Clostridiaceae: SGB43072; Lachnospiraceae: SGB41239, SGB41411, SGB41535, SGB41609, and SGB43003; and Ruminococcaceae: SGB43546).

The cecum content levels of XANA, PICO, and QUIN, all end products of the Kyn pathway (Figure 3D), showed significant correlations with the cecum microbiota, suggesting a local influence of the gut microbiota on Kyn degradation. In addition, strong correlations were observed with serum PICO and QUIN, suggesting that the influence of the gut microbiota on Kyn metabolite production could come out at a systemic level. Moreover, 3HAA, the intermediate metabolite between 3H-kyn and PICO or QUIN, also showed numerous correlations not only in the SI content and tissue but also in the cecum content, while 3H-kyn had a very poor correlation profile. This suggests that the cecum microbiota could particularly stimulate 3H-kyn transformation into XANA or 3HAA.

Surprisingly, except for ILA and tryptamine, metabolites from the indole pathway in the cecal and SI content exhibited relatively poor correlation profiles (Figure 3E), while the indoles are directly produced by the microbial activity in the gut lumen. It could be that different species have redundant activities related with indole metabolism or it could be related to the highly dynamic nature of the luminal level of indoles that are constantly

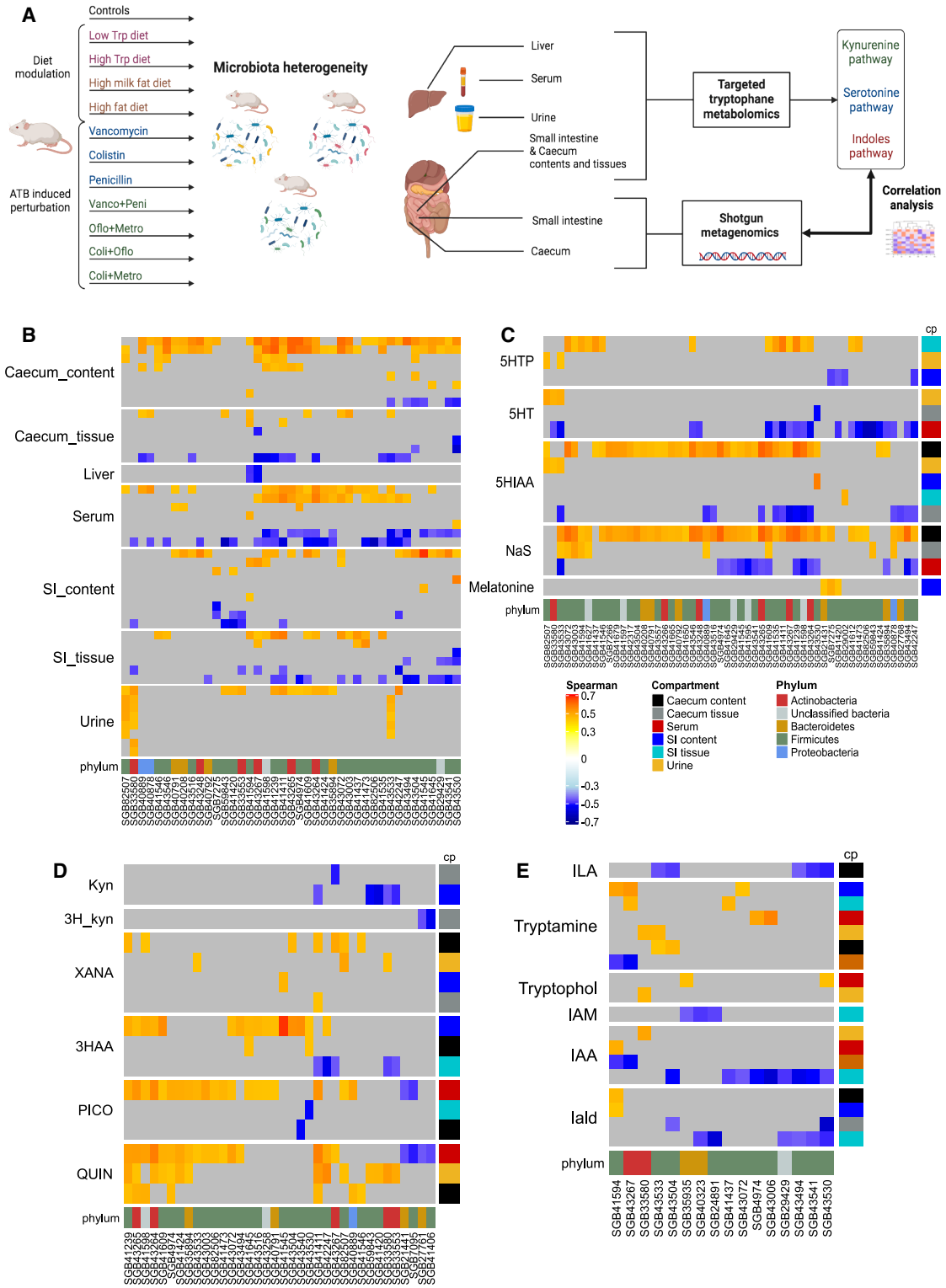

Figure 3. The cecal microbiota shows complex correlations with tryptophan metabolites, especially in the cecum content and the serum

(A) Outline of the experiment. Mice were raised under various conditions to induce high microbiome heterogeneity, increasing our power to find relevant associations between Trp metabolism and the gut microbiome. Mice were fed with a low- or high-Trp diet (n = 3 each), fed with a high-milk-fat diet or high-fat diet (n = 3 each), or received different antibiotic treatments (n = 3 per antibiotics. Vanco: vancomycin, Peni: penicillin, Oflo: ofloxacin, Metro: metronidazole, Coli: colistin). The rest of the mice were bred as controls of each condition (n = 15 in total). The gut microbiota was sampled in the cecum and the small intestine

(legend continued on next page)

transformed by gut microbiota members and absorbed. In this perspective, indole levels in tissues and in serum are likely more stable and thus more prone to identify correlation signals. This is the case for IAM, IAA, and IAld in the SI tissue, and to a lesser extent in the serum for tryptamine and tryptophol. It can be noticed that tryptamine showed particularly rich and positive correlation profiles compared to the other indole derivatives, suggesting that this metabolite exhibits specific and maybe more direct links with some SGBs. More precisely, serum tryptamine was significantly correlated with both Bacillota (SGB43006, SGB4974, and SGB41675) and Bacteroidota (formerly Bacteroidetes), from Rikenellaceae (SGB40208), Odoribacteraceae (SGB40791, whose closest reference genome is GCA_009935865, *Odoribacter* sp. *Z80*, average distance 0.23), and other unknown families (SGB40368, SGB21428, and SGB35953). Tryptamine in the other compartments was significantly correlated to either Bacillota or Actinomycetes. Interestingly, urine tryptamine was significantly correlated to SGB43533 and SGB82507—*Anaerotruncus colihominis* from the Ruminococcaceae family, and SGB33580—*Atopobiaceae bacterium* FL090493. These three SGBs were also the only ones to be significantly and positively correlated with urine 5HT, 5HTP, and 5HIAA, which further suggests a link with 5HT production. SGB43533 was also positively correlated to cecum content tryptamine, along with SGB43504, an unknown SGB whose closest reference genome is GCA_000403435—*Oscillibacter* sp. *1–3* genome assembly (average distance 0.17). The number of bacterial species that are known for being able to produce tryptamine is growing, comprising *Ruminococcus gnavus* and *Clostridium sporogenes,*[35,36] and potentially *Blautia hansenii, Clostridium asparagiforme, Tyzzerella nexilis,* and *Enterococcus faecalis*.[36] However, further research is needed to confirm and identify tryptamine producers, like the ones suggested here by our findings. All significant (FDR adjusted <0.1) individual SGBs' correlations with Trp metabolites as well as their identification can be found in Table S1.

Taken together, these observations suggest that the link between the gut microbiota and Trp metabolism is complex, possibly because the various metabolic transformations of Trp metabolism happen in different compartments or because microbial interactions or redundancy in microbial activity could be involved in Trp metabolism.

Grouping SGBs into co-abundance guilds can better explain measurements of certain metabolites

Based on the complexity of these correlation patterns, and the fact that several microbes are likely collaborating regarding the same functions, we thought to find a method to regroup SGBs into units that could better explain the levels of Trp metabolites than single bacterium. For this purpose, we used cecum metagenomics data to group SGBs into "guilds" according to their co-abundance.[37] Hierarchical clustering identified 44 guilds, regrouping 2–11 taxa, represented in Figure 4A. The SGB composition of guilds can be found in Table S2.

To investigate how these guilds correlated with the metabolites, we first summed SGB abundances for each guild and correlated it to the metabolite abundances (Figure 4B). Interestingly, some guilds were significantly correlated to metabolite abundance, although none of their individual SGBs considered individually were correlated with it, as guild 1 with cecum content I3S, for example (negative correlation). This could be due to the fact that FDR correction in guilds' analysis is done with fewer features compared to individual SGBs, but it could also be that grouping microbial species according to their co-abundance can reveal correlations that were unapparent at the single-species level. Interestingly, guild 1 contained Bacillota (SGB41553, SGB42491); Actinomycetes of the Bifidobacteriaceae (SGB17278, *Bifidobacterium animalis*), Propionibacteriaceae (SGB16955), and Streptomycetaceae families (SGB44472); and Bacteroidota (SGB21428, SGB1863, *Bacteroides caecimuris*). Of note, *Bifidobacterium animalis* is known for producing ILA,[39] which leads to other degrading products than I3S. Thus, it is possible that this bacterial community is able to influence the indole pathway, and especially Trp degradation into other indole derivatives than those leading to I3S.

In addition, it is interesting to note that neither guild 42 nor any of its SGBs showed any significant correlation with Trp metabolites. This guild was composed of four Bacillota, namely, *Staphylococcus nepalensis* (SGB7839), *Jeotgalicoccus halotolerans* (SGB24956), *Mammaliicoccus lentus* (SGB7817), and *Ligilactobacillus murinus* (SGB7077), and of one Actinobacteria (SGB17126—*Corynebacterium ammoniagenes*). This suggests that these bacterial species do not take part in or have a minor influence on Trp metabolism. Interestingly, guild 3, composed of *Lactobacillus taiwanensis* (SGB7040) and *Limosilactobacillus reuteri* (SGB7095), was found to be negatively correlated with both serum PICO and QUIN, suggesting that these species may negatively influence the transformation of 3HAA in these metabolites.

We observed that before adjusting for FDR, correlation with the whole guild was often statistically stronger than with any individual microbe of the guild, reinforcing the value of this approach (Figure 4B, detailed results of the guild's correlations with Trp metabolites can be found in Table S3). However, the *p* value decrease was generally moderate. In three guilds only, the *p* value decrease reached 10- to 100-fold: guild 1 with cecum

and analyzed using metagenomics. Metabolomics was performed on samples from the small intestine content and tissue, the cecum content and tissue, the liver, the serum, and the urine of mice. Microbial abundances deduced from metagenomics were then correlated to the metabolites of each compartment using Spearman's correlation.

(B) Spearman's correlations between abundances of SGBs from the cecum microbiota and Trp metabolite levels, split by compartment. Only SGBs involved in more than 3 significant correlations are shown. Identifiers of SGBs are indicated at the bottom.

(C–E) Spearman's correlation analysis between abundances of SGBs from the cecal microbiota and Trp metabolite levels, split by metabolites from the serotonin (C), kynurenine (D), and indole (E) pathways. Only significant correlations (*p* adjusted <0.1 after correction for the FDR, using the Benjamini-Hochberg procedure) are shown and colored from blue to red according to their correlation coefficient. Rows and columns are hierarchically clustered using complete linkage and Euclidean distance. Only SGBs involved in more than one significant correlation are shown. Identifiers of SGBs are indicated at the bottom.

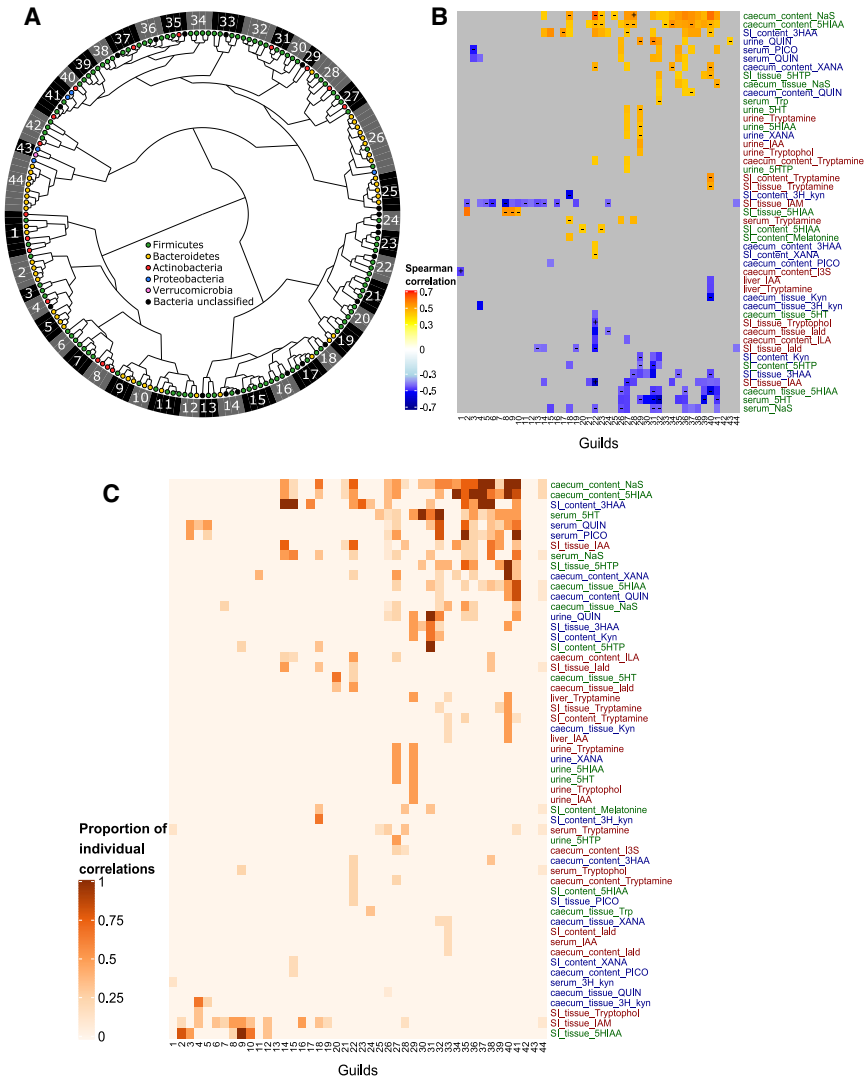

Figure 4. Grouping SGBs into co-abundance guilds improves Spearman's correlation with certain Trp metabolites

(A) Representation of the guild tree using GraPhlAn software.[38] Guild construction (see STAR Methods for details): Spearman's correlation coefficients were calculated on relative abundance values for each pair of SGBs, and a dissimilarity matrix was constructed using 1-correlation coefficient as filling values. This matrix was then used to perform hierarchical clustering following Ward's method, which minimizes the within-cluster variance according to the sum-of-squares criterion. The resulting clustering tree was analyzed from the root node with a procedure to choose the optimal number of clusters. Specifically, at each node, a Permanova test was used to test if the two child clades were significantly different. If the two clades were indeed statistically different (p value <0.05), the exploration continued in the two corresponding branches independently, repeating at each new node the Permanova statistical test. If the two clades were not significantly different, they were considered to form a unique guild and the exploration was stopped for that branch. In the end, a partition of the SGB pool was formed, with significantly different guilds that do not necessarily correspond to a fixed height in the tree. This whole procedure is a re-factoring of the methodology by Wu et al., 2021.[37]

(B) Heatmap of Spearman's correlations between guilds and metabolites. Only metabolites with which at least one guild was correlated significantly are represented, and only significant correlations (p adjusted <0.1 after correction for the FDR, using the Benjamini-Hochberg procedure) are colored from blue to red according to their correlation coefficient. Rows were hierarchically clustered using complete linkage and Euclidean distance. A symbol indicates correlations for which the guild was better in terms of p value than any of its individual SGB. The symbol depends on the strength of p value reduction (ratio between the minimal p value among the SGBs composing the guild and the p value of the guild). −: less than 10, +: between 10 and 100.

(C) Proportion of SGBs from each guild correlated with a given metabolite. For each guild, the number of individual SGBs significantly correlated with each of the metabolites was computed. Correlations were considered significant if p adjusted <0.1 after correction for the FDR, using the Benjamini-Hochberg procedure. Then for each guild, the counts were normalized by their total number of SGBs. Normalized counts were colored with a scale from 0 to 1 (beige to brown), 1 meaning that all the SGBs of the guild are individually correlated with the metabolite. Rows were hierarchically clustered using complete linkage and Euclidean distance.

content I3S (negative correlation), guild 22 with both IAA and tryptophol from the SI tissue (negative correlations), and guild 28 with cecum content NaS. Of note, guild 22 was mainly composed of Bacillota of the Ruminococcaceae (SGB43530 and SGB43504) and Lachnospiraceae (SGB41549) families. An explanation for this moderate improvement of correlation strength could be that a guild contains distinct subunits that are not all linked to the production of the metabolite, so summing them partially neutralizes the potential associations with Trp metabolism. A second possibility might be that the level of a given metabolite is impacted by several guilds in parallel.

To explore these two hypotheses, we plotted for each guild its proportion of SGBs significantly correlated with a given metabolite (Figure 4C). Some metabolites were very specific to a guild, meaning that they correlated with most SGBs of the guild and with almost no members of other guilds. This was the case for guild 18 with SI content 3H-kyn, for example (negative correlation). This guild was also significantly and positively correlated with SI content 3HAA, which suggests that this bacterial community could particularly participate (directly or indirectly) in the degradation of 3H-kyn to 3HAA in the SI.

Also, some guilds were specific to a metabolite, meaning that most of their SGBs only correlated with one metabolite. For example, SGBs of guild 2 mostly correlated with SI tissue 5HIAA, and this guild had the strongest correlation with this metabolite (estimate = 0.59, FDR adjusted = 0.008). Of note, SI

tissue 5HIAA can be considered as an indicator of local 5HT production in the SI, as after its production and release by ECs, 5HT can either join the systemic circulation or be re-uptaken, via SERT, by nearby enterocytes, which will then degrade it to 5HIAA. Interestingly, guild 2 was composed of four SGBs of the Muribaculaceae family (unknown species SGB27767 and SGB27763, SGB2088—*Muribaculum intestinale*, and SGB21584—*Paramuribaculum intestinale*) and one unknown Bacillota (SGB41432). This suggests that this bacterial community might have a specific behavior regarding 5HT production and re-uptake by enterocytes in the SI. Of note, the abundance of the *Muribaculum* genus was previously found to be increased after oral gavage with 5HT in mice,[40] which suggests that 5HT production and degradation into 5HIAA could promote growth in these species.

In contrast, most of the time, SGBs individually correlated to a given metabolite, such as serum 5HT, were shared between several guilds. Most SGBs of guilds 30 and 32 were correlated with this metabolite, which suggests that these SGBs might share a similar behavior with respect to 5HT metabolism, making them potentially interesting to regroup. Moreover, except guilds 30 and 32, several other guilds contained SGBs correlated with serum 5HT but in smaller proportion, which further suggests that these guilds could be composed of multiple microbial subunits that globally follow the same abundance dynamics but have distinct behaviors regarding 5HT metabolism. More precisely, we found that guild 32 was strongly and negatively correlated with serum 5HT (estimate = 0.62, FDR adjusted = 0.005). This guild was mainly composed of unknown SGBs from the Lachnospiraceae family (SGB59843, SGB41411, SGB41424, and SGB41473). It was shown that the colonization of GF mice with spore-forming bacteria, among which is the Lachnospiraceae family, promotes 5HT production via Tph1 activation, with elevated 5HT levels in the colon and serum,[10] which is inconsistent with our results. As these SGBs are unknown species, it is possible that they belong to a species that exhibits specific behaviors regarding Tph1 activation. Of note, guild 32 was also positively correlated with SI tissue 5HTP (estimate = 0.47, FDR adjusted = 0.05), the direct product of the action of Tph1 on Trp. Thus, a hypothesis to explain these results could be that the Lachnospiraceae bacteria found in guild 32 can promote local 5HT production via Tph1 activation in the SI but then favor its local utilization rather than its passage in the systemic circulation. Similar results were obtained with guild 39.

When we mapped SGBs' guild membership to the individual correlations (Figures 3B and S4), we noticed that the correlation profiles of the guilds were very much intertwined, in agreement with previous remarks. Furthermore, considering that in this figure the SGBs are arranged according to their correlation profile with the metabolites, some guilds look more alike, as it is the case for guilds 35 and 36, or guilds 14 and 22, suggesting that they might contain microbial subunits having a common behavior toward Trp metabolism.

Taken together, these results suggest that co-abundance guilds of SGBs could outline multiple types of communities in relation to how their SGBs are linked to Trp metabolism. This further suggests that there is a need to investigate how these microbial communities interact regarding Trp metabolism and explore which bacterial functions underlie these interactions.

Functional analysis sheds light on bacterial functions that could be involved in Trp metabolism

To further explore potential functional links between guilds and Trp metabolites, we correlated metabolite, individual SGB and guild abundances with EC enzyme and MetaCyc pathways abundances.

We did not find any significant correlations between guild or SGB and MetaCyc pathways abundances related to Trp metabolism (Tables S4, S5). However, we found that abundance of tryptophanase (EC 4.1.99.1), catalyzing the transformation of Trp into indole, was very strongly and positively correlated with guild 26 (estimate = 0.94, FDR adjusted = 4.3×10^{-19}, Figure 5A). Each of the 11 SGBs of this guild was strongly and significantly correlated with tryptophanase when taken individually. Four of them belonged to the Rikenellaceae family (SGB40208, SGB40196, SGB35894, and SGB40190), the first 3 having the strongest correlations of all SGBs with tryptophanase, which is consistent with other findings.[41,42] Of note, some other SGBs of guild 26 that significantly correlated with tryptophanase belonged to the Odoribacteraceae family.

Then, we found that amidase (EC 3.5.1.4), an enzyme catalyzing the transformation of IAM into IAA, was very strongly correlated with guild 31 (estimate = 0.96, FDR adjusted = 1.1×10^{-22}, Figure 5B). This guild contained SGB42247 of the Erysipelotrichaceae family, an *Adlercreutzia muris* SGB from the Eggerthellaceae family (SGB33553), and an unknown species of the Lachnospiraceae family (SGB41420). Surprisingly, the Erysipelotrichaceae family was previously found to be negatively associated with IAA and indole-3-propionic acid.[43,44] In our study, we did not find any significant correlation between indole metabolites and guild 31 or any of its SGBs. This could be that IAA is quickly further metabolized into other compounds *in vivo*, or that the link of this guild with amidase is rather related to the use of this enzyme in other pathways, as it is not specific to the Trp metabolism. However, guild 8, composed of 4 SGBs from the Eggerthellaceae family (SGB33554—*Adlercreutzia mucosicola,* SGB14802—*Adlercreutzia caecimuris,* SGB42958—*Enterorhabdus* sp. *P55*, and SGB86230, an unknown species), had the strongest negative correlation with SI tissue IAM (estimate = −0.56, FDR adjusted = 0.021), which could be an indirect indicator of IAA production. In addition, SGB29002 from guild 9, an unknown SGB with GCA_004793885—*Dubosiella muris* as closest reference genome (average distance 0.01), and SGB39153—*Turicibacter* sp. *TS3* from guild 10, both from the Erysipelotrichaceae family, are also significantly and negatively correlated with SI tissue IAM (estimate = −0.47 and −0.53, FDR adjusted = 0.07 and 0.03 respectively). These results suggest that bacteria of the Eggerthellaceae, especially the *Adlercreutzia* genus, and Erysipelotrichaceae families could participate in the degradation of IAM into IAA, possibly through amidase expression.

Finally, we found that the guilds that were the most strongly correlated with arylformamidase (EC 3.5.1.9), the enzyme catalyzing the transformation of Trp into Kyn, were guilds 14, 15, 22, 37, and 38 (estimates = 0.70, 0.62, 0.63, 0.62, and 0.73 and

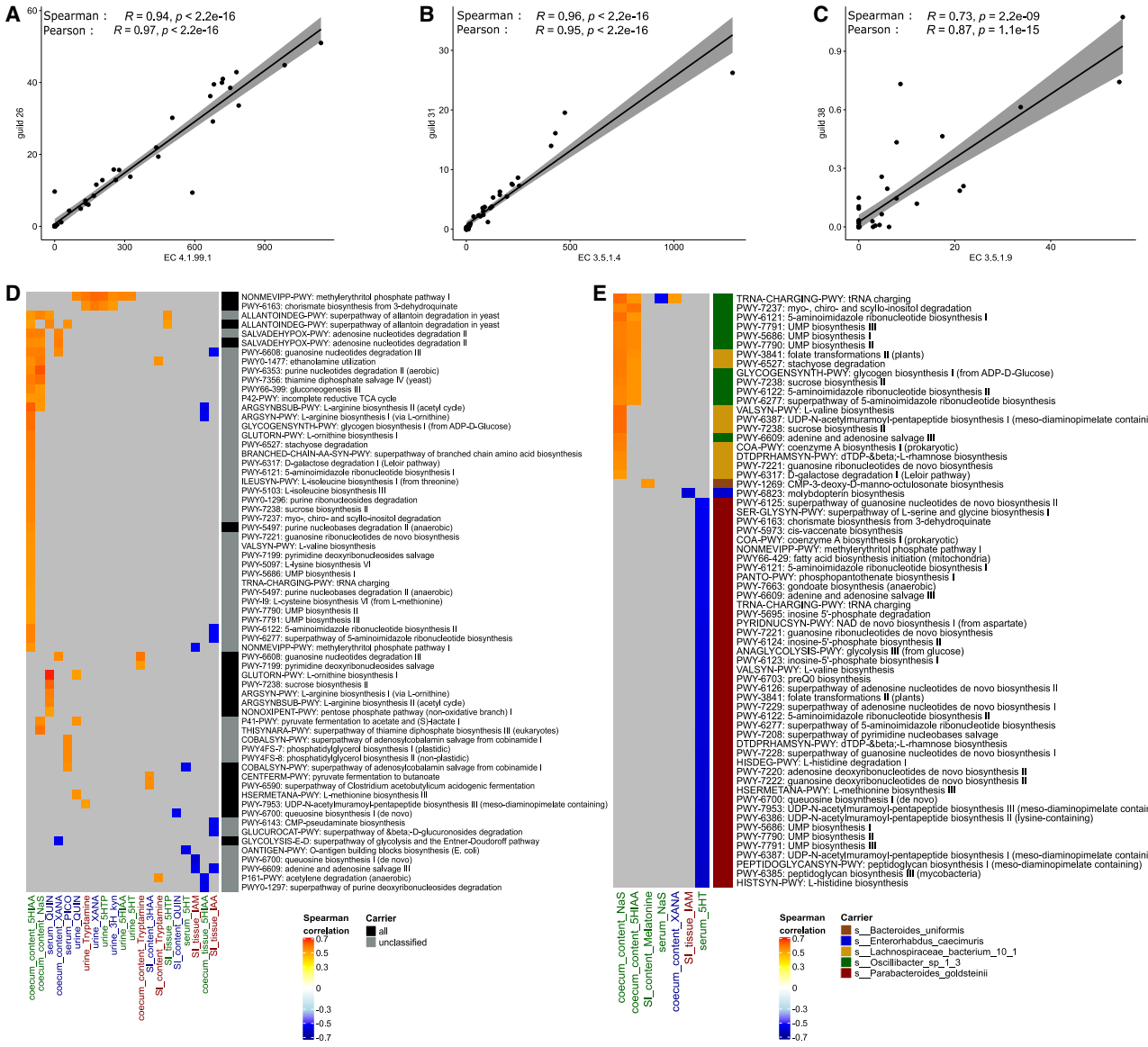

Figure 5. Functional analysis sheds light on bacterial functions that could be involved in Trp metabolism

(A–C) Correlation plot between guild 26 and EC 4.1.99.1 (A), guild 31 and EC 3.5.1.4 (B), and guild 38 and EC 3.5.1.9 (C). For each plot, abundances of SGBs of the corresponding guild were summed and correlated with the abundance of the corresponding EC enzyme. Spearman's and Pearson's correlation estimates are shown.

(D and E) Heatmap of Spearman's correlations between metabolites and MetaCyc pathways either carried by all bacteria or all unclassified bacteria (D), or by specific bacterial species (E). Only metabolites with at least one significant correlation with MetaCyc pathways are shown. Only significant correlations (p adjusted <0.1 after correction for the FDR, using the Benjamini-Hochberg procedure) are colored from blue to red according to their correlation coefficient. Rows and columns are hierarchically clustered using complete linkage and Euclidean distance.

FDR adjusted = 4.6×10^{-7}, 2.2×10^{-5}, 1.4×10^{-5}, 2.0×10^{-5}, 9.0×10^{-8}, respectively, Figures 5C and S5). These guilds were also significantly and positively correlated with SI content 3HAA, which could indirectly support a positive link with Kyn production from Trp. Guild 15 had the strongest correlation with SI content 3HAA (estimate = 0.54, FDR adjusted = 0.02) and was composed of unknown SGBs from the Lachnospiraceae (SGB41554, SGB41618 and SGB41545) and Ruminococcaceae families (SGB63182 and SGB43540). Of note, SGB41545 had the strongest correlation with SI content 3HAA among individual SGBs (estimate = 0.68, FDR adjusted = 0.002). Guilds 14, 22, 37, and 38 were mainly composed of unknown Bacillota, mostly from the Lachnospiraceae, Ruminococcaceae, or other unknown families, and some of these SGBs (SGB43504 in guild 22, SGB43516 in guild 37, and SGB43494 in guild 38) had as closest reference genome GCA_000403435—*Oscillibacter* sp. *1–3* genome assembly (average distance: 0.17, 0.20, and 0.14, respectively). Interestingly, the *Oscillibater* genera were previously found to be

positively associated with Kyn, 5HT, and 5HTP plasma levels.[45] These results suggest a potential role of the Lachnospiraceae and Ruminococcaceae bacterial families regarding the production of Kyn from Trp via arylformamidase expression, and possibly the *Oscillibacter* genera.

Guild 18, which was mentioned above for its potential responsibility in the transformation of 3H-kyn into 3HAA in the SI, was also significantly correlated to the relative abundance of arylformamidase (estimate = 0.60, FDR adjusted = 5.5×10^{-5}). This suggests that bacteria of this guild could have the capacity to transform Trp into Kyn and promote its further degradation from 3H-kyn to 3HAA. This guild contained a *Dorea* species (SGB7275), *Romboutsia ilealis* (SGB24891), and an unclassified bacterium (SGB41595). Consistently, bacteria of the *Dorea* genus are known for increasing the secretion of interferon γ by T cells,[43,46] a cytokine that was found to induce the production of Kyn in various types of cells through IDO activity,[47,48] and the *Romboutsia* genus was found to be associated with arylformamidase function.[13] Interestingly, it was also found to be associated with the nitrilase function catalyzing the formation of IAA,[13] which is consistent with our finding as this *Romboutsia ilealis* SGB was significantly and negatively correlated with both SI tissue IAld and IAM, which can be an indirect sign of IAA production in the SI.

Contrary to guilds and SGBs, we found several significant correlations between MetaCyc pathways and metabolite abundances (Figures 5D and 5E). First, we found that serum QUIN was strongly and positively correlated with the L-ornithine biosynthesis I pathway (Spearman estimate = 0.69, FDR adjusted = 0.005), just as urine QUIN, and with the L-arginine biosynthesis I (via L-ornithine) and L-arginine biosynthesis II (acetyl cycle) pathways. Similarly, cecum content 5HIAA was positively correlated with the L-ornithine biosynthesis I and L-arginine biosynthesis I and II pathways carried by unclassified SGBs. Interestingly, cecum tissue 5HIAA was negatively correlated with the L-arginine biosynthesis I and II pathways carried by unclassified SGBs. Little is known about the effects of bacterial production and utilization of arginine on the intestinal inflammatory response, but some studies have found that oral supplementation with L-arginine could reduce intestinal inflammation in IBD (Inflammatory bowel disease), thanks to its transformation by host intestinal cells, for example, into L-ornithine.[49,50] Thus, it is possible that the degradation of Trp through both the Kyn and serotonin pathways participates in this mechanism.

Also, both serum PICO and serum QUIN were positively correlated with the superpathway of allantoin degradation in yeast, and cecum content XANA, with the adenosine nucleotide degradation II and guanosine nucleotide degradation III pathways, both leading to the formation of urate, the substrate for the production of allantoin under the action of reactive oxygen species. Interestingly, simultaneously increased blood levels of allantoin and Kyn[51,52] or its derivatives QUIN and PICO[52–55] were previously found in various pathological situations. These results support a potential link between bacterial allantoin metabolism and Kyn production and further degradation into QUIN or PICO, especially during host inflammatory response.

Importantly, we did not detect any enzymes involved in the serotonin pathway in our dataset, which is consistent with the fact that the production of serotonin metabolites is due to the host activity. However, we found numerous significant correlations between metabolites of the serotonin pathway and bacterial pathways or EC enzymes. First, urine 5HIAA was significantly and positively correlated with the methylerythritol phosphate pathway I (Spearman estimate = 0.56, FDR adjusted = 0.04). This pathway was also positively correlated with urine 5HT, urine 5HTP, and cecum content 5HIAA and negatively correlated with serum 5HT. It leads to the production of isopentenyl pyrophosphate and dimethylallyl pyrophosphate, which are both isoprenoid precursors. Interestingly, isoprenoids are known for being able to modulate levels of neurotransmitters like 5HT in the central nervous system, particularly by interacting with $5HT1_A$ and $5HT3_A$ receptors.[56–59] However, little is known about their effects on peripheral serotonin production, and it is possible that the gut microbiota influence 5HT production locally in the gut through the activation of the methylerythritol phosphate pathway I. Interestingly, this pathway was also significantly and positively correlated with urine tryptamine, XANA, and QUIN, which further suggests a link with the Kyn and indole pathways.

Most correlations with serum 5HT were negative and with pathways carried by *Parabacteroides goldsteinii*. Among the strongest correlations, we found the L-histidine biosynthesis and L-methionine biosynthesis III pathways and several pathways related to peptidoglycan biosynthesis, namely, peptidoglycan biosynthesis I and III and UDP-N-acetylmuramoyl-pentapeptide biosynthesis I, II, and III, UDP-N-acetylmuramoyl-pentapeptide being a component of peptidoglycan. Cecum content NaS was also positively correlated with the UDP-N-acetylmuramoyl-pentapeptide biosynthesis I pathway carried by an unknown SGB (*Lachnospiraceae_bacterium_10_1*). We also found associations between metabolites of the serotonin pathway and the biosynthesis of lipopolysaccharide (LPS) components. Indeed, serum 5HT was negatively correlated to the dTDP-L-rhamnose biosynthesis pathway carried by *Parabacteroides goldsteinii* and to the *E. coli* O-antigen building block biosynthesis pathway carried by unclassified bacteria, and SI content melatonin, positively with the CMP-3-deoxy-D-manno-octulosonate biosynthesis pathway carried by *Bacteroides uniformis*. These results suggest that detection of cell membrane components of bacteria like peptidoglycan and LPS by the host could regulate local 5HT production and degradation.

Taken together, functional analysis provides useful data to better understand which bacterial functions could underlie the interactions between the different bacterial communities of the gut microbiota, with regard to Trp metabolism.

DISCUSSION

In this study, we investigated the links between the gut microbiota and Trp metabolism. Besides showing the massive impact of the gut microbiota on Trp metabolism, we identified specific correlations between SGBs and Trp metabolites through the building of co-abundance guilds and analysis of functional data.

First, comparing levels of Trp metabolites between GF and CV mice, we showed that not only the indole pathway but also the Kyn and serotonin pathways were impacted by the microbiota,

although the latter are known to be mostly due to host metabolism. This suggests that the activity of the gut microbiota could directly or indirectly regulate host metabolism. Surprisingly in our study, 5HT levels in the serum did not differ between GF and CV mice, unlike previous findings that either compared serum 5HT[10,60] or plasma 5HT[61] levels. An explanation could be that as 5HT is transported and released by blood platelets, 5HT levels in the serum can vary according to the degree of platelet activation and can significantly differ between serum and plasma. Another study found that serum 5HT levels did not differ between GF and CV mice when analyzing together samples from male and female mice, while they differed when comparing male GF and CV mice but not female.[62] As our experiment only used female mice, this could be another explanation for these results.

As a second step, we analyzed how metagenomics-derived microbial abundances correlated with Trp metabolites at the taxa level. Compared to the SI, the large intestine has a greater abundance and richness of microbes.[63,64] Although Trp metabolism is active in both the large intestine and SI, little is known about the differential impact of the microbiota on these two compartments. We showed that the cecal microbiota had richer and stronger correlation patterns with Trp metabolites, suggesting a preponderant role over the ileal microbiota. However, we also found that the cecal microbiota correlated well with metabolites sampled from the SI content or tissues. Therefore, the direct or indirect effect of the gut microbiota on Trp metabolism appears to rely on complex mechanisms, and it is likely that intense microbial activity within the cecum has remote effects on the whole organism, including the SI. Microbial abundances also showed strong correlation profiles in other systemic compartments like the serum, supporting the hypothesis of a remote influence of cecal microbial activity on Trp metabolism.

Since relative abundances of individual taxa often displayed similar correlation patterns regarding Trp metabolism, and as microbes are known for interacting into ecological niches showing redundant behaviors, we grouped them into co-abundance guilds using metagenomics data from the cecum. These co-abundance guilds exhibited improved correlations with some Trp metabolites. However, it also appeared that different guilds comprised SGBs sharing similar correlation profiles regarding Trp metabolism. This is understandable as guilds are based on abundances deduced from all DNA material found in the samples, reflecting the global abundance of the microbes and not only their behavior relative to Trp metabolism.

Combining the results of the progressive approach from individual SGBs to guilds, with functional analysis, we have highlighted new possible interactions between the gut microbiome and Trp metabolism.

First, we highlighted potential actors of Kyn metabolism and production from Trp. Indeed, we have identified *Romboutsia ilealis* and the *Dorea* genus as candidates for promoting the degradation of 3H-kyn into 3HAA in the SI content, and degrading Trp into Kyn via arylformamidase expression. We also identified many unknown SGBs that could carry this enzyme, mainly from the Lachnospiraceae and Ruminococcaceae families, with some SGBs having as closest reference genome a member of the *Oscillibacter* genus. Interestingly, the *Oscillibacter* genus was found to be increased in mice under low-Trp diet, along with elevated inflammatory markers like interleukin (IL)-6 and IL-1a,[65] and to be associated with inflammation and increased gut permeability.[66,67] However, contradictory results were found in other studies, which found this genus to be enriched in the healthy group in comparison to pathological NAFLD (Nonalcoholic fatty liver disease) group[68] or IBD group,[69,70] or in the inactive Crohn disease group in comparison to the active Crohn disease group.[71] All these elements predominantly support the hypothesis that members of the gut microbiota, and especially the SGBs that we have identified, could mediate gut inflammation by modulating the production of Kyn from Trp, possibly through arylformamidase expression. However, there is still a need to better characterize these SGBs, as well as how they interact and to what extent they participate in the intensity of the gut inflammatory response.

Our results also highlighted potentially interesting links between the gut microbiota and systemic levels of PICO and QUIN. We have identified *Lactobacillus taiwanensis* and *Limosilactobacillus reuteri* to be negatively correlated with both serum PICO and QUIN, and guild 26, containing several members of the Rikenellaceae family, to be positively correlated. In addition, we have found that QUIN in the serum and urine was correlated to pathways related to L-arginine and L-ornithine biosynthesis and that serum PICO and QUIN levels were positively correlated to pathways related to allantoin metabolism. Interestingly, allantoin is known for being a biomarker of oxidative stress,[72–75] and it has been suggested in a mouse model of IBD that allantoin was a biomarker of gut inflammation.[76] Allantoin blood levels were also found to be correlated with fecal calprotectin levels in children with Crohn disease.[77] These elements support a potential link between host inflammatory response mediated by Kyn production and further degradation into QUIN or PICO, and allantoin metabolism by the gut microbiota.

Then, our results concerning the serotonin pathway suggest that microbial activity can positively influence local 5HT production and has an impact on systemic levels of serotonin metabolites. Importantly, except for the specific and positive correlation between SI tissue 5HIAA and SGBs of the Muribaculaceae family, our analysis with individual SGBs and guilds has shown that bacterial links with serotonin metabolism are likely very complex and intertwined, suggesting that multiple bacterial behaviors could influence serotonin production and degradation by the host.

However, functional analysis sheds light on how bacterial activity could be linked to host production of 5HT and its derivatives. In particular, we have found that metabolites of the serotonin pathway, not only serum 5HT but also to a lesser extent cecum content NaS and SI content melatonin, were strongly correlated with pathways related to peptidoglycan and LPS production. Yet, several studies have shown that peptidoglycan fragments are recognized by NOD1 and NOD2 receptors inside intestinal cells[78–80] and that NOD1 activation inhibits SERT and downregulates its expression, which could induce an increase in extracellular 5HT levels.[81,82] Peptidoglycan fragments are also recognized by TLR2 and TLR4 receptors, which also regulate SERT expression.[81] LPS can also be recognized by TLR4, and thus downregulate SERT expression.[81,83,84] These results support the hypothesis that detection by the host of cell

membrane components of bacteria like peptidoglycan and LPS could regulate local 5HT production by ECs. Furthermore, we did not find any significant correlations between 5HIAA in any of the compartments and pathways related to components of bacterial cell wall like LPS or peptidoglycan, which further suggests that the reaction triggered by bacterial detection in host intestinal cells could favor the transformation of serotonin into NaS and melatonin rather than 5HIAA.

Finally, we identified new potential actors of the indole pathway. For instance, we identified *Anaerotruncus colihominis* regarding tryptamine production, *Bifidobacterium animalis* and *Bacteroides caecimuris* regarding I3S production, and the Eggerthellaceae, especially the *Adlercreutzia* genus *(A. muris, A. mucosicola)*, and Erysipelotrichaceae families regarding IAA production through amidase expression.

Some of our results also support the hypothesis that indole production is an indirect way for microbes to influence both the serotonin and Kyn pathways. Indeed, we have found that some SGBs positively correlated with levels of urine tryptamine were also positively correlated with urine 5HT, 5HTP, and 5HIAA. Yet, it was shown that in the colon, tryptamine stimulates 5HT secretion via 5-HT4R[85] and 5HT biosynthesis via trace amine-associated receptor 1 (TAAR1) activation.[86] Thus, it is possible that these SGBs could promote 5HT production via tryptamine synthesis.

In addition, guild 26 was not only strongly and positively correlated with tryptophanase but also negatively with serum 5HT and positively with serum PICO and serum QUIN, suggesting that indole production through tryptophanase expression can influence both the serotonin and Kyn pathways. As an example of how these pathways could interact, it was previously suggested that *Alistipes,* a genus of the Rikenellaceae family, could take part in the physiopathology of depression by favoring the transformation of Trp into indole and by producing LPS, which induces an inflammatory state favoring the Kyn pathway via IDO1 activation[87,88] and could regulate 5HT production when detected by the host as mentioned above.

Thus, focusing on microbial DNA-derived abundances to study microbial communities establishes a fundamental foundation for the understanding of microbial interactions with the host, but other aspects of the host-microbiota dialog in Trp metabolism should further be considered. It is known that Trp metabolism, and especially the Kyn and serotonin pathways, is also greatly influenced by the host activity. It would be interesting to integrate host transcriptomics data into this approach in order to have an insight into the holobiont, or the host-microbiome system.[89] These aspects could also help answer the question of causality of the correlations found in our analysis. Moreover, bacteria are not the only members of the gut microbiota to take part in Trp metabolism, and there is emerging evidence that viruses, archaea, and eukaryotes are also at play.[90] This is important from an ecological point of view, as these populations of organisms are constantly regulating each other's growth and expression profiles through metabolite production. Finally, Trp metabolism might also depend on the local environment of the gut, and so, especially on diet. Indeed, it was shown that different dietary sources of Trp influenced AhR activation patterns.[91] It was found that a high-fat diet in mice induced an upregulation of the Kyn pathway through an increase of IDO expression[92–94] and a decrease in production of some indole derivatives.[93,95–97] In addition, a study found that 5HIAA levels in colon and serum were decreased under high-fat diet in mice with insulin resistance,[98] while others found increased 5HT levels in the gut[97,99] and plasma.[97] On the contrary, diets rich in fibers were found to downregulate the production of Kyn via an increased production of SCFA (Short-chain fatty acids) like butyrate[93,100] and increase the levels of indole derivatives like IAA, IAld, ILA, and IPA.[101–103] Finally, Trp supplementation was found to increase the production of indole derivatives,[102] while Trp deficiency was found to decrease the levels of metabolites from the indole,[104,105] kynurenin, and serotonin[105] pathways. Thus, it is possible that diet has influenced the measures in our study. However, the effects of diet can be mediated by microbial activity, and we purposely used different diets and antibiotic treatments to induce microbiome heterogeneity and thus potentially highlight specific bacterial actors that are more active under certain conditions.

To conclude, we have shown that the activity of the cecal microbiota plays a major role in Trp metabolism. Grouping SGBs into guilds according to their co-abundances, we have improved the understanding of the links between the gut microbiota and Trp metabolites and highlighted the complexity of microbial interactions regarding Trp metabolism. Including functional analysis, we have highlighted potential mechanisms of the host-microbiota dialog that will need to be confirmed and explored experimentally, which could pave the way for the development of therapeutic guilds.

Limitations of the study

The main limitation of our study is the lack of experimental confirmation of the links between specific bacterial taxa and Trp metabolites that we identified *in silico*. Further study will be required to address it. A second limitation is the fact that our study has been performed in mice only. It would be important to confirm the results in humans.

RESOURCE AVAILABILITY

Lead contact

Further information and requests for resources and reagents should be directed to and will be fulfilled by the lead contact, Harry Sokol (harry.sokol@gmail.com).

Materials availability

This study did not generate new unique reagents.

Data and code availability

- Raw sequence data are accessible under NCBI-SRA BioProject: PRJEB52043
- This paper does not report original code, but it is available from the lead contact upon request.
- Any additional information required to reanalyze the data reported in this work paper is available from the lead contact upon request.

ACKNOWLEDGMENTS

The authors wish to thank the staff of the INRAE Infectiology of Fishes and Rodents Facility (IERP-UE907, Jouy-en-Josas Research Center, France) and ANAXEM (germ-free animal facility, MICALIS, Jouy-en-Josas Research

Center, France), where animal experiments have been performed. H.S. received funding from the European Research Council (ERC) under the European Union's Horizon 2020 Research and Innovation Program (ERC-2016-StG-71577) and from Agence Nationale de Recherche (ANR-20-CE14-0005-1).

AUTHOR CONTRIBUTIONS

M.L. and H.S. designed the study. M.L. and P.M. performed the bioinformatics analyses. N.R., A.L., and J.P. performed the experiments. M.L, H.S., M.B., and N.S. interpreted the results and drafted the manuscript. All the authors reviewed the manuscript, gave critical feedback and approved the manuscript.

DECLARATION OF INTERESTS

H.S. reports lecture fee, board membership, or consultancy from Amgen, Fresenius, IPSEN, Actial, Astellas, Danone, THAC, Biose, BiomX, Eligo, Immusmol, Adare, Nestle, Ferring, MSD, Bledina, Pfizer, Biocodex, BMS, Bromatech, Gilead, Janssen, Mayoli, Roche, Sanofi, Servier, Takeda, and Abbvie; has stocks from Enterome Bioscience; and is co-founder of Exeliom Biosciences.

STAR★METHODS

Detailed methods are provided in the online version of this paper and include the following:

- KEY RESOURCES TABLE
- EXPERIMENTAL MODEL AND SUBJECT DETAILS
  - Germ-free vs. conventionalized mice
  - Mice with heterogeneous gut microbiome
- METHOD DETAILS
  - Nucleic acids extraction
  - Sequencing
- QUANTIFICATION AND STATISTICAL ANALYSIS
  - Metagenomes' downstream analysis
  - Targeted quantitative metabolomics
  - EC enzymes and Metacyc pathways analysis
  - Statistical analyses
  - Guilds' construction

SUPPLEMENTAL INFORMATION

Supplemental information can be found online at https://doi.org/10.1016/j.isci.2025.113751.

Received: March 14, 2025
Revised: June 9, 2025
Accepted: October 9, 2025
Published: October 14, 2025

REFERENCES

1. Kalbermatter, C., Fernandez Trigo, N., Christensen, S., and Ganal-Vonarburg, S.C. (2021). Maternal Microbiota, Early Life Colonization and Breast Milk Drive Immune Development in the Newborn. Front. Immunol. *12*, 683022.
2. Zheng, D., Liwinski, T., and Elinav, E. (2020). Interaction between microbiota and immunity in health and disease. Cell Res. *30*, 492–506. https://doi.org/10.1038/s41422-020-0332-7.
3. Pickard, J.M., Zeng, M.Y., Caruso, R., and Núñez, G. (2017). Gut microbiota: Role in pathogen colonization, immune responses, and inflammatory disease. Immunol. Rev. *279*, 70–89. https://doi.org/10.1111/imr.12567.
4. Oliphant, K., and Allen-Vercoe, E. (2019). Macronutrient metabolism by the human gut microbiome: major fermentation by-products and their impact on host health. Microbiome *7*, 91. https://doi.org/10.1186/s40168-019-0704-8.
5. Lamas, B., Richard, M.L., Leducq, V., Pham, H.-P., Michel, M.-L., Da Costa, G., Bridonneau, C., Jegou, S., Hoffmann, T.W., Natividad, J.M., et al. (2016). CARD9 impacts colitis by altering gut microbiota metabolism of tryptophan into aryl hydrocarbon receptor ligands. Nat. Med. *22*, 598–605. https://doi.org/10.1038/nm.4102.
6. Agus, A., Planchais, J., and Sokol, H. (2018). Gut Microbiota Regulation of Tryptophan Metabolism in Health and Disease. Cell Host Microbe *23*, 716–724. https://doi.org/10.1016/j.chom.2018.05.003.
7. Natividad, J.M., Agus, A., Planchais, J., Lamas, B., Jarry, A.C., Martin, R., Michel, M.-L., Chong-Nguyen, C., Roussel, R., Straube, M., et al. (2018). Impaired Aryl Hydrocarbon Receptor Ligand Production by the Gut Microbiota Is a Key Factor in Metabolic Syndrome. Cell Metab. *28*, 737–749.e4. https://doi.org/10.1016/j.cmet.2018.07.001.
8. Lamas, B., Hernandez-Galan, L., Galipeau, H.J., Constante, M., Clarizio, A., Jury, J., Breyner, N.M., Caminero, A., Rueda, G., Hayes, C.L., et al. (2020). Aryl hydrocarbon receptor ligand production by the gut microbiota is decreased in celiac disease leading to intestinal inflammation. Sci. Transl. Med. *12*, eaba0624. https://doi.org/10.1126/scitranslmed.aba0624.
9. Mawe, G.M., and Hoffman, J.M. (2013). Serotonin signalling in the gut—functions, dysfunctions and therapeutic targets. Nat. Rev. Gastroenterol. Hepatol. *10*, 473–486. https://doi.org/10.1038/nrgastro.2013.105.
10. Yano, J.M., Yu, K., Donaldson, G.P., Shastri, G.G., Ann, P., Ma, L., Nagler, C.R., Ismagilov, R.F., Mazmanian, S.K., and Hsiao, E.Y. (2015). Indigenous Bacteria from the Gut Microbiota Regulate Host Serotonin Biosynthesis. Cell *161*, 264–276. https://doi.org/10.1016/j.cell.2015.02.047.
11. Clarke, G., Grenham, S., Scully, P., Fitzgerald, P., Moloney, R.D., Shanahan, F., Dinan, T.G., and Cryan, J.F. (2013). The microbiome-gut-brain axis during early life regulates the hippocampal serotonergic system in a sex-dependent manner. Mol. Psychiatry *18*, 666–673. https://doi.org/10.1038/mp.2012.77.
12. Kennedy, P.J., Cryan, J.F., Dinan, T.G., and Clarke, G. (2017). Kynurenine pathway metabolism and the microbiota-gut-brain axis. Neuropharmacology *112*, 399–412. https://doi.org/10.1016/j.neuropharm.2016.07.002.
13. Vazquez-Medina, A., Rodriguez-Trujillo, N., Ayuso-Rodriguez, K., Marini-Martinez, F., Angeli-Morales, R., Caussade-Silvestrini, G., Godoy-Vitorino, F., and Chorna, N. (2024). Exploring the interplay between running exercises, microbial diversity, and tryptophan metabolism along the microbiota-gut-brain axis. Front. Microbiol. *15*, 1326584. https://doi.org/10.3389/fmicb.2024.1326584.
14. Lamas, B., Natividad, J.M., and Sokol, H. (2018). Aryl hydrocarbon receptor and intestinal immunity. Mucosal Immunol. *11*, 1024–1038. https://doi.org/10.1038/s41385-018-0019-2.
15. Brazier, J.S., Duerden, B.I., Hall, V., Salmon, J.E., Hood, J., Brett, M.M., McLAUCHLIN, J., and George, R.C. (2002). Isolation and identification of Clostridium spp. from infections associated with the injection of drugs: experiences of a microbiological investigation team. J. Med. Microbiol. *51*, 985–989. https://doi.org/10.1099/0022-1317-51-11-985.
16. Dong, F., and Perdew, G.H. (2020). The aryl hydrocarbon receptor as a mediator of host-microbiota interplay. Gut Microbes *12*, 1859812. https://doi.org/10.1080/19490976.2020.1859812.
17. Rosser, E.C., Piper, C.J.M., Matei, D.E., Blair, P.A., Rendeiro, A.F., Orford, M., Alber, D.G., Krausgruber, T., Catalan, D., Klein, N., et al. (2020). Microbiota-Derived Metabolites Suppress Arthritis by Amplifying Aryl-Hydrocarbon Receptor Activation in Regulatory B Cells. Cell Metab. *31*, 837–851.e10. https://doi.org/10.1016/j.cmet.2020.03.003.
18. Manzella, C.R., Ackerman, M., Singhal, M., Ticho, A.L., Ceh, J., Alrefai, W.A., Saksena, S., Dudeja, P.K., and Gill, R.K. (2020). Serotonin Modulates AhR Activation by Interfering with CYP1A1-Mediated Clearance of AhR Ligands | Cell Physiol Biochem. Cell. Physiol. Biochem. *54*, 126–141.

19. Ahmed, S., Sparidans, R.W., Lu, J., Mihaila, S.M., Gerritsen, K.G.F., and Masereeuw, R. (2022). A robust, accurate, sensitive LC–MS/MS method to measure indoxyl sulfate, validated for plasma and kidney cells. Biomed. Chromatogr. *36*, e5307. https://doi.org/10.1002/bmc.5307.

20. Pommerolle, P., Caillard, P., Louvet, L., Slama, M., Maizel, J., Boullier, A., Chatelain, D., Spicher, P., Choukroun, G., Kamel, S., et al. (2024). Elevation of serum indoxyl-sulfate in mice with normal kidney function triggers cardiac and vascular dysfunctions. Nephrol. Dial. Transplant. *39*, gfae0691095. https://doi.org/10.1093/ndt/gfae069.1095.

21. Shimada, Y., Kinoshita, M., Harada, K., Mizutani, M., Masahata, K., Kayama, H., and Takeda, K. (2013). Commensal Bacteria-Dependent Indole Production Enhances Epithelial Barrier Function in the Colon. PLoS One *8*, e80604. https://doi.org/10.1371/journal.pone.0080604.

22. Sun, C.-Y., Li, J.-R., Wang, Y.-Y., Lin, S.-Y., Ou, Y.-C., Lin, C.-J., Wang, J.-D., Liao, S.-L., and Chen, C.-J. (2021). Indoxyl sulfate caused behavioral abnormality and neurodegeneration in mice with unilateral nephrectomy. Aging *13*, 6681–6701. https://doi.org/10.18632/aging.202523.

23. Hou, H., Horikawa, M., Narita, Y., Jono, H., Kakizoe, Y., Izumi, Y., Kuwabara, T., Mukoyama, M., and Saito, H. (2023). Suppression of Indoxyl Sulfate Accumulation Reduces Renal Fibrosis in Sulfotransferase 1a1-Deficient Mice. Int. J. Mol. Sci. *24*, 11329. https://doi.org/10.3390/ijms241411329.

24. Adesso, S., Magnus, T., Cuzzocrea, S., Campolo, M., Rissiek, B., Paciello, O., Autore, G., Pinto, A., and Marzocco, S. (2017). Indoxyl Sulfate Affects Glial Function Increasing Oxidative Stress and Neuroinflammation in Chronic Kidney Disease: Interaction between Astrocytes and Microglia. Front. Pharmacol. *8*, 370. https://doi.org/10.3389/fphar.2017.00370.

25. Pina-Beltran, B., Dimitrov, D., McKay, N., Giot, M., Zdráhal, Z., Potěšil, D., Pustka, V., Peinado-Izaguerri, J., Saez-Rodriguez, J., Poitevin, S., and Burtey, S. (2025). Unveiling the role of sex in the metabolism of indoxyl sulfate and apixaban. Sci. Rep. *15*, 6075. https://doi.org/10.1038/s41598-025-90405-5.

26. Hung, S.C., Kuo, K.L., Wu, C.C., and Tarng, D.C. (2017). Indoxyl Sulfate: A Novel Cardiovascular Risk Factor in Chronic Kidney Disease. J. Am. Heart Assoc. *6*, e005022. https://doi.org/10.1161/JAHA.116.005022.

27. Morgan, E.W., Dong, F., Annalora, A.J., Murray, I.A., Wolfe, T., Erickson, R., Gowda, K., Amin, S.G., Petersen, K.S., Kris-Etherton, P.M., et al. (2023). Contribution of Circulating Host and Microbial Tryptophan Metabolites Toward Ah Receptor Activation. Int. J. Tryptophan Res. *16*, 11786469231182510. https://doi.org/10.1177/11786469231182510.

28. Xie, Y., Li, X., Meng, Q., Li, J., Wang, X., Zhu, L., Wang, W., and Li, X. (2024). Interplay between gut microbiota and tryptophan metabolism in type 2 diabetic mice treated with metformin. Microbiol. Spectr. *12*, e0029124. https://doi.org/10.1128/spectrum.00291-24.

29. Zhang, X., Gan, M., Li, J., Li, H., Su, M., Tan, D., Wang, S., Jia, M., Zhang, L., and Chen, G. (2020). Endogenous Indole Pyruvate Pathway for Tryptophan Metabolism Mediated by IL4I1. J. Agric. Food Chem. *68*, 10678–10684. https://doi.org/10.1021/acs.jafc.0c03735.

30. Sadik, A., Somarribas Patterson, L.F., Öztürk, S., Mohapatra, S.R., Panitz, V., Secker, P.F., Pfänder, P., Loth, S., Salem, H., Prentzell, M.T., et al. (2020). IL4I1 Is a Metabolic Immune Checkpoint that Activates the AHR and Promotes Tumor Progression. Cell *182*, 1252–1270.e34. https://doi.org/10.1016/j.cell.2020.07.038.

31. Zeitler, L., and Murray, P.J. (2023). IL4i1 and IDO1: Oxidases that control a tryptophan metabolic nexus in cancer. J. Biol. Chem. *299*, 104827. https://doi.org/10.1016/j.jbc.2023.104827.

32. Sprunck, S., Jacobsen, H.-J., and Reinard, T. (1995). Indole-3-lactic acid is a weak auxin analogue but not an anti-auxin. J. Plant Growth Regul. *14*, 191–197. https://doi.org/10.1007/BF00204911.

33. Ludwig-Müller, J. (2011). Auxin conjugates: their role for plant development and in the evolution of land plants. J. Exp. Bot. *62*, 1757–1773. https://doi.org/10.1093/jxb/erq412.

34. Rampey, R.A., LeClere, S., Kowalczyk, M., Ljung, K., Sandberg, G., and Bartel, B. (2004). A family of auxin-conjugate hydrolases that contributes to free indole-3-acetic acid levels during Arabidopsis germination. Plant Physiol. *135*, 978–988. https://doi.org/10.1104/pp.104.039677.

35. Williams, B.B., Van Benschoten, A.H., Cimermancic, P., Donia, M.S., Zimmermann, M., Taketani, M., Ishihara, A., Kashyap, P.C., Fraser, J.S., and Fischbach, M.A. (2014). Discovery and characterization of gut microbiota decarboxylases that can produce the neurotransmitter tryptamine. Cell Host Microbe *16*, 495–503. https://doi.org/10.1016/j.chom.2014.09.001.

36. Sugiyama, Y., Mori, Y., Nara, M., Kotani, Y., Nagai, E., Kawada, H., Kitamura, M., Hirano, R., Shimokawa, H., Nakagawa, A., et al. (2022). Gut bacterial aromatic amine production: aromatic amino acid decarboxylase and its effects on peripheral serotonin production. Gut Microbes *14*, 2128605..

37. Wu, G., Zhao, N., Zhang, C., Lam, Y.Y., and Zhao, L. (2021). Guild-based analysis for understanding gut microbiome in human health and diseases. Genome Med. *13*, 22. https://doi.org/10.1186/s13073-021-00840-y.

38. Asnicar, F., Weingart, G., Tickle, T.L., Huttenhower, C., and Segata, N. (2015). Compact graphical representation of phylogenetic data and metadata with GraPhlAn. PeerJ *3*, e1029. http://segatalab.cibio.unitn.it/tools/graphlan/.

39. Sakurai, T., Odamaki, T., and Xiao, J.Z. (2019). Production of Indole-3-Lactic Acid by Bifidobacterium Strains Isolated fromHuman Infants. Microorganisms *7*, 340. https://doi.org/10.3390/microorganisms7090340.

40. Sanidad, K.Z., Rager, S.L., Carrow, H.C., Ananthanarayanan, A., Callaghan, R., Hart, L.R., Li, T., Ravisankar, P., Brown, J.A., Amir, M., et al. (2023). Gut bacteria-derived serotonin promotes immune tolerance in early life. Preprint at bioRxiv. https://doi.org/10.1101/2022.09.25.509428.

41. Gryp, T., Huys, G.R.B., Joossens, M., Van Biesen, W., Glorieux, G., and Vaneechoutte, M. (2020). Isolation and Quantification of Uremic Toxin Precursor-Generating Gut Bacteria in Chronic Kidney Disease Patients. Int. J. Mol. Sci. *21*, 1986. https://doi.org/10.3390/ijms21061986.

42. Jaglin, M., Rhimi, M., Philippe, C., Pons, N., Bruneau, A., Goustard, B., Daugé, V., Maguin, E., Naudon, L., and Rabot, S. (2018). Indole, a Signaling Molecule Produced by the Gut Microbiota, Negatively Impacts Emotional Behaviors in Rats. Front. Neurosci. *12*, 216. https://doi.org/10.3389/fnins.2018.00216.

43. Riazati, N., Kable, M.E., Newman, J.W., Adkins, Y., Freytag, T., Jiang, X., and Stephensen, C.B. (2022). Associations of microbial and indoleamine-2,3-dioxygenase-derived tryptophan metabolites with immune activation in healthy adults. Front. Immunol. *13*, 917966. https://doi.org/10.3389/fimmu.2022.917966.

44. Xiao, L., Yan, J., Yang, T., Zhu, J., Li, T., Wei, H., and Chen, J. (2021). Fecal Microbiome Transplantation from Children with Autism Spectrum Disorder Modulates Tryptophan and Serotonergic Synapse Metabolism and Induces Altered Behaviors in Germ-Free Mice. mSystems *6*, e0134320. https://doi.org/10.1128/msystems.01343-20.

45. Chen, L., Chen, D.-Q., Liu, J.-R., Zhang, J., Vaziri, N.D., Zhuang, S., Chen, H., Feng, Y.-L., Guo, Y., and Zhao, Y.-Y. (2019). Unilateral ureteral obstruction causes gut microbial dysbiosis and metabolome disorders contributing to tubulointerstitial fibrosis. Exp. Mol. Med. *51*, 1–18. https://doi.org/10.1038/s12276-019-0234-2.

46. Schirmer, M., Smeekens, S.P., Vlamakis, H., Jaeger, M., Oosting, M., Franzosa, E.A., Ter Horst, R., Jansen, T., Jacobs, L., Bonder, M.J., et al. (2016). Linking the Human Gut Microbiome to Inflammatory Cytokine Production Capacity. Cell *167*, 1125–1136.e8. https://doi.org/10.1016/j.cell.2016.10.020.

47. Alberati-Giani, D., Ricciardi-Castagnoli, P., Köhler, C., and Cesura, A.M. (1996). Regulation of the Kynurenine Metabolic Pathway by Interferon-γ in Murine Cloned Macrophages and Microglial Cells. J. Neurochem. *66*, 996–1004. https://doi.org/10.1046/j.1471-4159.1996.66030996.x.

48. Saito, K., Chen, C.Y., Masana, M., Crowley, J.S., Markey, S.P., and Heyes, M.P. (1993). 4-Chloro-3-hydroxyanthranilate, 6-chlorotryptophan and norharmane attenuate quinolinic acid formation by interferon-gamma-stimulated monocytes (THP-1 cells). Biochem. J. *291*, 11–14.

49. Li, J.Y., Guo, Y.C., Zhou, H.F., Yue, T.T., Wang, F.X., Sun, F., and Wang, W.Z. (2023). Arginine metabolism regulates the pathogenesis of inflammatory bowel disease - PMC. Nutr. Rev. *81*, 578–586. https://pmc.ncbi.nlm.nih.gov/articles/PMC10086623/.

50. Fritz, J.H. (2013). Arginine Cools the Inflamed Gut - PMC. Infect. Immun. *81*, 3500–3502. https://pmc.ncbi.nlm.nih.gov/articles/PMC3811762/.

51. Gironès, N., Carbajosa, S., Guerrero, N.A., Poveda, C., Chillón-Marinas, C., and Fresno, M. (2014). Global Metabolomic Profiling of Acute Myocarditis Caused by Trypanosoma cruzi Infection. PLoS Negl Trop Dis. *8*, e3337.. https://journals.plos.org/plosntds/article?id=10.1371/journal.pntd.0003337.

52. Charkoftaki, G., Aalizadeh, R., Santos-Neto, A., Tan, W.Y., Davidson, E. A., Nikolopoulou, V., Wang, Y., Thompson, B., Furnary, T., Chen, Y., et al. (2023). An AI-powered patient triage platform for future viral outbreaks using COVID-19 as a disease model. Hum. Genomics *17*, 80. https://doi.org/10.1186/s40246-023-00521-4.

53. Abbiss, H., Maker, G.L., and Trengove, R.D. (2019). Metabolomics Approaches for the Diagnosis and Understanding of Kidney Diseases - PMC. Metabolites. *9*, 34. https://pmc.ncbi.nlm.nih.gov/articles/PMC6410198/.

54. Gong, W., Jia, J., Zhang, B., Mi, S., Zhang, L., Xie, X., Guo, H., Shi, J., and Tu, C. (2017). Frontiers | Serum Metabolomic Profiling of Piglets Infected with Virulent Classical Swine Fever Virus. Front. Microbiol. *8*, 731.. https://www.frontiersin.org/journals/microbiology/articles/10.3389/fmicb.2017.00731/full.

55. Cihan, M., Doğan, Ö., Ceran Serdar, C., Altunçekiç Yıldırım, A., Kurt, C., and Serdar, M.A. (2022). Kynurenine pathway in Coronavirus disease (COVID-19): Potential role in prognosis. J. Clin. Lab. Anal. *36*, e24257. https://doi.org/10.1002/jcla.24257.

56. Rodriguez Araujo, N., Fabiani, C., Mazzarini Dimarco, A., Bouzat, C., and Corradi, J. (2020). Orthosteric and Allosteric Activation of Human 5-HT3A Receptors. Biophys. J. *119*, 1670–1682. https://doi.org/10.1016/j.bpj.2020.08.029.

57. Komiya, M., Takeuchi, T., and Harada, E. (2006). Lemon oil vapor causes an anti-stress effect via modulating the 5-HT and DA activities in mice. Behav. Brain Res. *172*, 240–249. https://doi.org/10.1016/j.bbr.2006.05.006.

58. Ziemba, P.M., Schreiner, B.S., Flegel, C., Herbrechter, R., Stark, T.D., Hofmann, T., Hatt, H., Werner, M., and Gisselmann, G. (2015). Activation and modulation of recombinantly expressed serotonin receptor type 3A by terpenes and pungent substances - ScienceDirect. Biochem. Biophys. Res. Commun. *467*, 1090–1096. https://www.sciencedirect.com/science/article/abs/pii/S0006291X1530591X.

59. Cox-Georgian, D., Ramadoss, N., Dona, C., and Basu, C. (2019). Therapeutic and Medicinal Uses of Terpenes | SpringerLink. In Medicinal Plants, N. Joshee, S. Dhekney, and P. Parajuli, eds. (Cham: Springer), pp. 333–359. https://link.springer.com/chapter/10.1007/978-3-030-31269-5_15.

60. Sjögren, K., Engdahl, C., Henning, P., Lerner, U.H., Tremaroli, V., Lagerquist, M.K., Bäckhed, F., and Ohlsson, C. (2012). The gut microbiota regulates bone mass in mice. J. Bone Miner. Res. *27*, 1357–1367. https://doi.org/10.1002/jbmr.1588.

61. Wikoff, W.R., Anfora, A.T., Liu, J., Schultz, P.G., Lesley, S.A., Peters, E. C., and Siuzdak, G. (2009). Metabolomics analysis reveals large effects of gut microflora on mammalian blood metabolites. Proc. Natl. Acad. Sci. USA *106*, 3698–3703. https://doi.org/10.1073/pnas.0812874106.

62. Lai, Y., Liu, C.-W., Yang, Y., Hsiao, Y.-C., Ru, H., and Lu, K. (2021). High-coverage metabolomics uncovers microbiota-driven biochemical landscape of interorgan transport and gut-brain communication in mice. Nat. Commun. *12*, 6000–6016. https://doi.org/10.1038/s41467-021-26209-8.

63. Booijink, C.C.G.M., El-Aidy, S., Rajilić-Stojanović, M., Heilig, H.G.H.J., Troost, F.J., Smidt, H., Kleerebezem, M., De Vos, W.M., and Zoetendal, E.G. (2010). High temporal and inter-individual variation detected in the human ileal microbiota. Environ. Microbiol. *12*, 3213–3227. https://doi.org/10.1111/j.1462-2920.2010.02294.x.

64. Zoetendal, E.G., Raes, J., van den Bogert, B., Arumugam, M., Booijink, C.C.G.M., Troost, F.J., Bork, P., Wels, M., de Vos, W.M., and Kleerebezem, M. (2012). The human small intestinal microbiota is driven by rapid uptake and conversion of simple carbohydrates. ISME J. *6*, 1415–1426. https://doi.org/10.1038/ismej.2011.212.

65. Yusufu, I., Ding, K., Smith, K., Wankhade, U.D., Sahay, B., Patterson, G. T., Pacholczyk, R., Adusumilli, S., Hamrick, M.W., Hill, W.D., et al. (2021). A Tryptophan-Deficient Diet Induces Gut Microbiota Dysbiosis and Increases Systemic Inflammation in Aged Mice. Int. J. Mol. Sci. *22*, 5005. https://doi.org/10.3390/ijms22095005.

66. Dai, J., Jiang, M., Wang, X., Lang, T., Wan, L., and Wang, J. (2024). Human-derived bacterial strains mitigate colitis via modulating gut microbiota and repairing intestinal barrier function in mice. BMC Microbiol. *24*, 96. https://doi.org/10.1186/s12866-024-03216-5.

67. Lam, Y.Y., Ha, C.W.Y., Campbell, C.R., Mitchell, A.J., Dinudom, A., Oscarsson, J., Cook, D.I., Hunt, N.H., Caterson, I.D., Holmes, A.J., and Storlien, L.H. (2012). Increased Gut Permeability and Microbiota Change Associate with Mesenteric Fat Inflammation and Metabolic Dysfunction in Diet-Induced Obese Mice. PLoS One *7*, e34233. https://doi.org/10.1371/journal.pone.0034233.

68. Jiang, W., Wu, N., Wang, X., Chi, Y., Zhang, Y., Qiu, X., Hu, Y., Li, J., and Liu, Y. (2015). Dysbiosis gut microbiota associated with inflammation and impaired mucosal immune function in intestine of humans with non-alcoholic fatty liver disease. Sci. Rep. *5*, 8096–8097. https://doi.org/10.1038/srep08096.

69. Pisani, A., Rausch, P., Bang, C., Ellul, S., Tabone, T., Marantidis Cordina, C., Zahra, G., Franke, A., and Ellul, P. (2022). Dysbiosis in the Gut Microbiota in Patients with Inflammatory Bowel Disease during Remission. Microbiol. Spectr. *10*, e0061622. https://doi.org/10.1128/spectrum.00616-22.

70. Mondot, S., Kang, S., Furet, J.P., Aguirre De Carcer, D., McSweeney, C., Morrison, M., Marteau, P., Doré, J., and Leclerc, M. (2011). Highlighting new phylogenetic specificities of Crohn's disease microbiota. Inflamm. Bowel Dis. *17*, 185–192. https://doi.org/10.1002/ibd.21436.

71. Metwaly, A., Dunkel, A., Waldschmitt, N., Raj, A.C.D., Lagkouvardos, I., Corraliza, A.M., Mayorgas, A., Martinez-Medina, M., Reiter, S., Schloter, M., et al. (2020). Integrated microbiota and metabolite profiles link Crohn's disease to sulfur metabolism. Nat. Commun. *11*, 4322. https://doi.org/10.1038/s41467-020-17956-1.

72. Kozlik, P., Hasikova, L., Stiburkova, B., Zavada, J., and Kalikova, K. (2020). Rapid and reliable HILIC-MS/MS method for monitoring allantoin as a biomarker of oxidative stress - ScienceDirect. Anal Biochem. *589*, 113509. https://www.sciencedirect.com/science/article/abs/pii/S0003269719310887.

73. Yardim-Akaydin, S., Sepici, A., Ozkan, Y., Simşek, B., and Sepici, V. (2006). Evaluation of allantoin levels as a new marker of oxidative stress in Behçet's disease. Scand. J. Rheumatol. *35*, 61–64. https://doi.org/10.1080/03009740510026878.

74. Kand'ár, R., and Záková, P. (2008). Allantoin as a marker of oxidative stress in hxuman erythrocytes. Clin. Chem. Lab. Med. *46*, 1270–1274. https://doi.org/10.1515/CCLM.2008.244.

75. Kand'ár, R., Záková, P., and Muzáková, V. (2006). Monitoring of antioxidant properties of uric acid in humans for a consideration measuring of levels of allantoin in plasma by liquid chromatography. Clin. Chim. Acta *365*, 249–256. https://www.researchgate.net/publication/7569623_Monitoring_of_antioxidant_properties_of_uric_acid_in_humans_for_a_consideration_measuring_of_levels_of_allantoin_in_plasma_by_liquid_chromatography.

76. Philippa, A.D., Donald, R.L., Michael, F.W., Dommels, Y., Butts, C., Rowan, D., Nicole, C.R., Helsby, N., Brian, L.B., Zhu, S., et al. (2008).

(PDF) Allantoin as A Biomarker of Inflammation in an Inflammatory Bowel Disease Mouse Model: NMR Analysis of Urine. Open Bioact. Compd. J. *1*, 1–6. https://doi.org/10.2174/1874847300801010001.

77. Kolho, K.L., Pessia, A., Jaakkola, T., de-Vos, W.M., and Velagapudi, V. (2017). Faecal and Serum Metabolomics in Paediatric Inflammatory Bowel Disease. J Crohns Colitis. *11*, 321–334. https://academic.oup.com/ecco-jcc/article-abstract/11/3/321/2631858?redirectedFrom=fulltext.
78. Bastos, P.A.D., Wheeler, R., and Boneca, I.G. (2021). Uptake, recognition and responses to peptidoglycan in the mammalian host - PMC. FEMS Microbiol. Rev. *45*, fuaa044.. https://www.ncbi.nlm.nih.gov/pmc/articles/PMC7794044/.
79. Stephen, E.G., Leonardo, H.T., Hervé, Mireille, Blanot, Didier, Ivo, G.B., Dana, J.P., Philippe, J.S., and Dominique, M.-L. (2003). Peptidoglycan Molecular Requirements Allowing Detection by Nod1 and Nod2 - ScienceDirect. J. Bio. Chem. *278*, 41702–41708. https://www.sciencedirect.com/science/article/pii/S0021925820826982.
80. Fernández-García, V., González-Ramos, S., Martín-Sanz, P., García-Del Portillo, F., Laparra, J.M., and Boscá, L. (2021). NOD1 in the interplay between microbiota and gastrointestinal immune adaptations. Pharmacol. Res. *171*, 105775. https://doi.org/10.1016/j.phrs.2021.105775.
81. Layunta, E., Buey, B., Emilio Mesonero, J., and Latorre, E. (2021). Frontiers | Crosstalk Between Intestinal Serotonergic System and Pattern Recognition Receptors on the Microbiota–Gut–Brain Axis. Front. Endocrinol. *12*, fendo.2021.748254. https://www.frontiersin.org/journals/endocrinology/articles/10.3389/fendo.2021.748254/full.
82. Layunta, E., Latorre, E., Forcén, R., Grasa, L., Plaza, M.A., Arias, M., Alcalde, A.I., and Mesonero, J.E. (2018). NOD1 downregulates intestinal serotonin transporter and interacts with other pattern recognition receptors. J. Cell. Physiol. *233*, 4183–4193. https://doi.org/10.1002/jcp.26229.
83. Mendoza, C., Matheus, N., Iceta, R., Mesonero, J.E., and Alcalde, A.I. (2009). Lipopolysaccharide induces alteration of serotonin transporter in human intestinal epithelial cells. Innate Immun. *15*, 243–250. https://doi.org/10.1177/1753425909104781.
84. Zhou, Q., and Nicholas Verne, G. (2022). Disruption of the Mucosal Serotonin Reuptake Transporter (SERT) Through Gut Dysbiosis. Gastroenterology *162*, 1833–1834. https://www.gastrojournal.org/article/S0016-5085(22)00291-8/fulltext.
85. Bhattarai, Y., Williams, B.B., Battaglioli, E.J., Whitaker, W.R., Till, L., Grover, M., Linden, D.R., Akiba, Y., Kandimalla, K.K., Zachos, N.C., et al. (2018). Gut Microbiota-Produced Tryptamine Activates an Epithelial G-Protein-Coupled Receptor to Increase Colonic Secretion. Cell Host Microbe *23*, 775–785.e5. https://doi.org/10.1016/j.chom.2018.05.004.
86. Zhai, L., Huang, C., Ning, Z., Zhang, Y., Zhuang, M., Yang, W., Wang, X., Wang, J., Zhang, L., Xiao, H., et al. (2023). Ruminococcus gnavus plays a pathogenic role in diarrhea-predominant irritable bowel syndrome by increasing serotonin biosynthesis. Cell Host Microbe *31*, 33–44.e5. https://doi.org/10.1016/j.chom.2022.11.006.
87. Dhaliwal, G.K. (2019). Alistipes: The influence of a commensal on anxiety and depression. Catal. Facets Biochem. Biomed. Sci. *3*, 2–10.
88. Parker, B.J., Wearsch, P., Veloo, A., and Rodriguez-Palacios, A. (2020). The Genus Alistipes: Gut Bacteria With Emerging Implications to Inflammation, Cancer, and Mental Health. Front. Immunol. *11*, 906.
89. Lim, R., Cabatbat, J.J.T., Martin, T.L.P., Kim, H., Kim, S., Sung, J., Ghim, C.-M., and Kim, P.-J. (2020). Large-scale metabolic interaction network of the mouse and human gut microbiota. Sci. Data *7*, 204. https://doi.org/10.1038/s41597-020-0516-5.
90. Zhang, J., Zhu, S., Ma, N., Johnston, L.J., Wu, C., and Ma, X. (2021). Metabolites of microbiota response to tryptophan and intestinal mucosal immunity: A therapeutic target to control intestinal inflammation. Med. Res. Rev. *41*, 1061–1088. https://doi.org/10.1002/med.21752.
91. Huang, Z., Schoones, T., Wells, J.M., Fogliano, V., and Capuano, E. (2021). Substrate-Driven Differences in Tryptophan Catabolism by Gut Microbiota and Aryl Hydrocarbon Receptor Activation. Mol. Nutr. Food Res. *65*, 2100092. https://doi.org/10.1002/mnfr.202100092.
92. Sun, P., Wang, M., Liu, Y.-X., Li, L., Chai, X., Zheng, W., Chen, S., Zhu, X., and Zhao, S. (2023). High-fat diet-disturbed gut microbiota-colonocyte interactions contribute to dysregulating peripheral tryptophan-kynurenine metabolism. Microbiome *11*, 154. https://doi.org/10.1186/s40168-023-01606-x.
93. Chajadine, M., Laurans, L., Radecke, T., Mouttoulingam, N., Al-Rifai, R., Bacquer, E., Delaroque, C., Rytter, H., Bredon, M., Knosp, C., et al. (2024). Harnessing intestinal tryptophan catabolism to relieve atherosclerosis in mice. Nat. Commun. *15*, 6390. https://doi.org/10.1038/s41467-024-50807-x.
94. Hyland, N.P., Cavanaugh, C.R., and Hornby, P.J. (2022). Emerging effects of tryptophan pathway metabolites and intestinal microbiota on metabolism and intestinal function. Amino Acids *54*, 57–70. https://doi.org/10.1007/s00726-022-03123-x.
95. Gao, K., Mu, C.L., Farzi, A., and Zhu, W.Y. (2020). Tryptophan Metabolism: A Link Between the Gut Microbiota and Brain. Adv. Nutr. *11*, 709–723. https://doi.org/10.1093/advances/nmz127.
96. Krishnan, S., Ding, Y., Saedi, N., Choi, M., Sridharan, G.V., Sherr, D.H., Yarmush, M.L., Alaniz, R.C., Jayaraman, A., and Lee, K. (2018). Gut Microbiota-Derived Tryptophan Metabolites Modulate Inflammatory Response in Hepatocytes and Macrophages. Cell Rep. *23*, 1099–1111. https://doi.org/10.1016/j.celrep.2018.03.109.
97. Fujisaka, S., Avila-Pacheco, J., Soto, M., Kostic, A., Dreyfuss, J.M., Pan, H., Ussar, S., Altindis, E., Li, N., Bry, L., et al. (2018). Diet, Genetics, and the Gut Microbiome Drive Dynamic Changes in Plasma Metabolites. Cell Rep. *22*, 3072–3086. https://doi.org/10.1016/j.celrep.2018.02.060.
98. Du, W., Jiang, S., Yin, S., Wang, R., Zhang, C., Yin, B.-C., Li, J., Li, L., Qi, N., Zhou, Y., and Ye, B.C. (2024). The microbiota-dependent tryptophan metabolite alleviates high-fat diet–induced insulin resistance through the hepatic AhR/TSC2/mTORC1 axis. Proc. Natl. Acad. Sci. *121*, e2400385121. https://doi.org/10.1073/pnas.2400385121.
99. Xu, M., Zhou, E.Y., and Shi, H. (2025). Tryptophan and Its Metabolite Serotonin Impact Metabolic and Mental Disorders via the Brain–Gut–Microbiome Axis: A Focus on Sex Differences. Cells *14*, 384. https://doi.org/10.3390/cells14050384.
100. Taleb, S. (2019). Tryptophan Dietary Impacts Gut Barrier and Metabolic Diseases. Front. Immunol. *10*, 2113. https://doi.org/10.3389/fimmu.2019.02113.
101. Hou, Y., Li, J., and Ying, S. (2023). Tryptophan Metabolism and Gut Microbiota: A Novel Regulatory Axis Integrating the Microbiome. Metabolites *13*, 1166. https://doi.org/10.3390/metabo13111166.
102. Sinha, A.K., Laursen, M.F., Brinck, J.E., Rybtke, M.L., Hjørne, A.P., Procházková, N., Pedersen, M., Roager, H.M., and Licht, T.R. (2024). Dietary fibre directs microbial tryptophan metabolism via metabolic interactions in the gut microbiota. Nat. Microbiol. *9*, 1964–1978. https://doi.org/10.1038/s41564-024-01737-3.
103. Huang, Z., Boekhorst, J., Fogliano, V., Capuano, E., and Wells, J.M. (2023). Impact of High-Fiber or High-Protein Diet on the Capacity of Human Gut Microbiota To Produce Tryptophan Catabolites. J. Agric. Food Chem. *71*, 6956–6966. https://doi.org/10.1021/acs.jafc.2c08953.
104. Konopelski, P., Konop, M., Gawrys, M., Piotr, P., and Ufnal, M. (2019). High-tryptophan Diet Reduces Weight Gain in Rats via Indole-3-propionic Acid, a Gut Microbiota Metabolite. FASEB J. *33*. https://doi.org/10.1096/fasebj.2019.33.1_supplement.592.7.
105. Rankin, L.C., Kaiser, K.A., De Los Santos-Alexis, K., Park, H., Uhlemann, A.-C., Gray, D.H.D., and Arpaia, N. (2023). Dietary tryptophan deficiency promotes gut RORγt+ Treg cells at the expense of Gata3+ Treg cells and alters commensal microbiota metabolism. Cell Rep. *42*, 112135. https://doi.org/10.1016/j.celrep.2023.112135.
106. Manghi, P., Blanco-Míguez, A., Manara, S., NabiNejad, A., Cumbo, F., Beghini, F., Armanini, F., Golzato, D., Huang, K.D., Thomas, A.M., et al. (2023).

MetaPhlAn 4 profiling of unknown species-level genome bins improves the characterization of diet-associated microbiome changes in mice. Cell Rep. *42*, 112464. https://doi.org/10.1016/j.celrep.2023.112464.

107. Blanco-Míguez, A., Beghini, F., Cumbo, F., McIver, L.J., Thompson, K.N., Zolfo, M., Manghi, P., Dubois, L., Huang, K.D., Thomas, A.M., et al. (2023). Extending and improving metagenomic taxonomic profiling with uncharacterized species using MetaPhlAn 4. Nat. Biotechnol. *41*, 1633–1644. https://doi.org/10.1038/s41587-023-01688-w.

108. Seemann, T. (2014). Prokka: rapid prokaryotic genome annotation. Bioinformatics *30*, 2068–2069. https://doi.org/10.1093/bioinformatics/btu153.

109. Steinegger, M., and Söding, J. (2017). MMseqs2 enables sensitive protein sequence searching for the analysis of massive data sets. Nat. Biotechnol. *35*, 1026–1028. https://doi.org/10.1038/nbt.3988.

110. Buuren, S.v., and Groothuis-Oudshoorn, K. (2011). mice: Multivariate Imputation by Chained Equations in R. J. Stat. Softw. *45*, 1–67. https://doi.org/10.18637/jss.v045.i03.

111. R Core Team (2020). R: A Language and Environment for Statistical Computing (R Foundation for Statistical Computing). https://www.R-project.org/.

112. Alboukadel, K. (2021). rstatix: Pipe-Friendly Framework for Basic Statistical Tests. R package version 0.7.0. https://CRAN.R-project.org/package=rstatix.

113. Oksanen, J., Guillaume Blanchet, F., Friendly, M., Kindt, R., Legendre, P., McGlinn, D., Minchin, P.R., O'Hara, R.B., Simpson, G.L., Solymos, P., et al. (2020). vegan: Community Ecology Package. R package version *2*, 5–7. https://CRAN.R-project.org/package=vegan.

114. Csardi, G., and Nepusz, T. (2006). The igraph software package for complex network research, InterJournal. Complex Syst. *1695*. https://igraph.org.

115. Beghini, F., McIver, L.J., Blanco-Míguez, A., Dubois, L., Asnicar, F., Maharjan, S., Mailyan, A., Manghi, P., Scholz, M., Thomas, A.M., et al. (2021). Integrating taxonomic, functional, and strain-level profiling of diverse microbial communities with bioBakery 3. eLife *10*, e65088. https://doi.org/10.7554/eLife.65088.

116. Quast, C., Pruesse, E., Yilmaz, P., Gerken, J., Schweer, T., Yarza, P., Peplies, J., and Glöckner, F.O. (2013). The SILVA ribosomal RNA gene database project: improved data processing and web-based tools. Nucleic Acids Res. *41*, D590–D596. https://doi.org/10.1093/nar/gks1219.

117. Pasolli, E., Asnicar, F., Manara, S., Zolfo, M., Karcher, N., Armanini, F., Beghini, F., Manghi, P., Tett, A., Ghensi, P., et al. (2019). Extensive Unexplored Human Microbiome Diversity Revealed by Over 150,000 Genomes from Metagenomes Spanning Age, Geography, and Lifestyle. Cell *176*, 649–662.e20. https://doi.org/10.1016/j.cell.2019.01.001.

118. Lefévre, A., Mavel, S., Nadal-Desbarats, L., Galineau, L., Attucci, S., Dufour, D., Sokol, H., and Emond, P. (2019). Validation of a global quantitative analysis methodology of tryptophan metabolites in mice using LC-MS. Talanta *195*, 593–598. https://doi.org/10.1016/j.talanta.2018.11.094.

119. Murtagh, F., and Legendre, P. (2014). Ward's Hierarchical Agglomerative Clustering Method: Which Algorithms Implement Ward's Criterion? J. Classif. *31*, 274–295. https://doi.org/10.1007/s00357-014-9161-z.

STAR★METHODS

KEY RESOURCES TABLE

REAGENT or RESOURCE	SOURCE	IDENTIFIER
Biological samples		
Stool samples from Germ Free mice	This paper	INRAe, Jouy-en-Josas, agreement C78-720
Stool samples from C57B6J mice	This paper	INRAe, Jouy-en-Josas, agreement C78-720
Critical commercial assays		
AllPrep DNA/RNA Mini Kit	Qiagen	80204
Agencourt AMPure XP	Beckman Coulter™	10136224
TURBO™ DNase	Thermo Fisher	AM2238
Agencourt RNAClean XP	Beckman Coulter™	NC0068576
Qubit RNA HS Assay Kit	Thermo Fisher	Q32852
Nextera XT DNA Library Preparation Kit	Illumina	FC-131-1096
Deposited data		
Raw sequencing data (metagenomics)	Manghi, P. et al.[106]	NCBI-SRA BioProject: PRJEB52043
Software and algorithms		
TrimGalore	NA	https://github.com/FelixKrueger/TrimGalore; RRID:SCR_011847
MetaPhlAn 4	Blanco-Míguez, A. et al.[107]	https://github.com/biobakery/MetaPhlAn
PROKKA	Seemann, T.[108]	https://github.com/tseemann/prokka; RRID:SCR_014732
MMseq2	Steinegger, M. & Söding, J.[109]	https://github.com/soedinglab/MMseqs2; RRID:SCR_026553
mice	Buuren S.v.&Groothuis-Oudshoorn K[110]	https://github.com/amices/mice; RRID:SCR_026363
stats	R Core Team[111]	https://www.rdocumentation.org/packages/stats/versions/3.6.2; RRID:SCR_025968
rstatix	Alboukadel Kassambara[112]	https://github.com/kassambara/rstatix; RRID:SCR_021240
Vegan	Jari Oksanen et al.[113]	https://github.com/vegandevs/vegan; RRID:SCR_011950
rigraph	Csardi G, & Nepusz T[114]	https://github.com/igraph/rigraph; RRID:SCR_021238
request	NA	https://github.com/request/request
HUMAnN 3.0	Beghini, F. et al.[115]	https://github.com/biobakery/humann; RRID:SCR_014620
Otherro		
SILVA database	Manghi, P. et al.[116]	v.132; RRID:SCR_006423
Uniparc	NA	https://www.uniprot.org/id-mapping; RRID:SCR_005818
Uniref. 90	NA	https://www.uniprot.org/help/uniref; RRID:SCR_010646
Metacyc pathways database	NA	https://metacyc.org/; RRID:SCR_007778
EC enzymes database	NA	https://enzyme.expasy.org/; RRID:SCR_002487

EXPERIMENTAL MODEL AND SUBJECT DETAILS

Germ-free vs. conventionalized mice

GF mice were raised in the specific pathogen-free facility ANAXEM at INRAe, Jouy-en-Josas, and half of them were conventionalized at six weeks. For conventionalization, fresh stools from C57B6J mice were immediately transferred to an anaerobic chamber, in

which the stools were suspended and diluted at 16 mg/mL in LYBHI medium (BD Difco, Le Pont de Claix, France) supplemented with cellobiose (1 mgml–1; Sigma C7252), maltose (1 mg ml–1; Sigma M5885), cysteine (0.5 mg ml–1; Sigma C6852), hemine (5 mg mL-1, Sigma H9039), K1 (0.2 μL mL-1, Sigma V3501) and K3 (16 mg mL-1, Sigma M5625) vitamins. Six-week-old GF mice were inoculated by oral gavage with 200 μL of the fecal suspension once daily for three consecutive days. After three weeks of implantation, the mice were sacrificed and samples were collected. In this study, only data from female mice were kept for analysis, to be consistent with the second mice experiment that used only female mice.

Mice with heterogeneous gut microbiome

The CM_mice_1 experiments were performed in the specific pathogen-free animal facility at IERP (INRAe, Jouy-en-Josas, agreement C78-720), in a temperature-controlled environment and with a strict 12h light/dark cycle. Animal experiments were performed according to the local ethical panel and the Ministére de l'Education Nationale, de l'Enseignement Supérieur et de la Recherche, France under agreement Apafis 19750-2019041014309428. Fifty females C57BL/6J from Janvier (France) were left for a minimum of 7 days acclimating (3–5 mice per cage/group). The gut microbiome of each group was then perturbed with one of the following challenges: vancomycin, colistin, penicillin, colistin + ofloxacin, vancomycin + penicillin, colistin + metronidazole, high-fat diet (Envigo TD.88137; 42% fat), high milk-fat diet (Envigo TD.97222, 38% fat), low Trp diet (Ssniff S9868-E020), high Trp diet (Ssniff S9868-E030), and control groups for each type of challenge (Envigo TD.97222 for high-fat diet, Ssniff S9868-E010 for low and high Trp diet). Antibiotics-treated mice were fed a conventional chow diet (Envigo TD.120508). Antibiotics were given in drinking water for 7 days at the following dosage: vancomycin, 0.5 g/L; metronidazole, 1 g/L; colistin, 1 g/L; penicillin, 1 g/L; ofloxacin, 0.25 g/L. Dietary interventions were maintained for 5 weeks before sacrifice.

METHOD DETAILS

Nucleic acids extraction

At the end of the perturbation, mice were euthanized, dissected and caecum and ileum aliquots were withdrawn and stored at −80 °C. For each sample, 100 mg of stool were carefully homogenized by vortexing with 110 μl of lysis buffer (TE buffer additioned with 20 mg/mL of proteinase K and 15 mg/mL of lysozyme) and incubated at room temperature for 10 min. DNA was extracted using the allPrep DNA/RNA Mini Kit (Qiagen) following the manufacturer's instructions. Eluted DNA was purified with Agencourt AMPure XP (Beckman Coulter) and quantified with Qubit dsDNA HS Assay Kit (Thermo Fisher Scientific).

Sequencing

Sequencing libraries were prepared using the Nextera XT DNA Library Preparation Kit (Illumina), following the manufacturer's guidelines. Sequencing was performed on a HiSeq2500 (Illumina) at the sequencing facility at University of Trento, Italy. Reads quality filtering was performed using trim_galore (parameters: –nextera –stringency 5 –length 75 –quality 20 –max_n 2 –trim-n), discarding all reads of quality less than 20 and shorter than 75 nucleotides. Filtered reads were then assigned to the C57BL/6J laboratory mouse genome (GCA_000001635.8), the PhiX genome and the SILVA database[116](v.132) for removal of host, contaminant and 16S material. Ninety-seven samples were obtained (26 classified as high-fat diet and 71 classified as normal chow), and 3.6 Bln. reads were produced (avg. per sample = 37 Mln. [2.8, 70]).

QUANTIFICATION AND STATISTICAL ANALYSIS

Metagenomes' downstream analysis

The 97 mouse samples were profiled using the recently described MetaPhlAn 4 pipeline[107] (version 4.0.0, Jan21 release) which incorporates in its database the species-level genome bins (SGB) system.[117] The SGBs are defined based both on reference genomes from isolated sequencing and on metagenomic-assembled genomes (MAGs), therefore allowing to quantify the relative contribution of both characterized and yet-to-be characterized SGBs. In total, the database encompassed more than one million metagenomic assembled genomes (MAGs) including 22,718 MAGs from 1,906 mice gut metagenomes,[106] that allowed the reconstruction of 540 completely uncharacterized microbial SGBs from mice' metagenomes only. In the present work, only profiles from samples that had a complementary metabolomics analysis in urine, ileal tissue, caecal tissue and liver were kept in the analysis (N = 95 samples).

Targeted quantitative metabolomics

The protocols for metabolomics were described before in Lefèvre et al., 2019.[118] Briefly, 20 Trp metabolites were quantified in the different compartments (the ileum tissue, the small intestine content, the caecum tissue, the caecum content, the liver, the serum and the urine) using liquid chromatography coupled with high resolution mass spectrometry (LC-HRMS).

As an example, we report protocols for blood samples analysis. The samples were collected after mice sacrifice, and were individually placed in Eppendorf tubes and kept at −80°C until analysis. Two protocols were used depending on the concentration of metabolites.

Protocol 1 : Metabolites were extracted from 100 μL of serum. After addition of the internal standards and 800 μL of MeOH, the samples were vortexed for 15s and homogenized at −20°C, for 30 min. After centrifugation at 15000x g for 10 min, 800 μL of

supernatant were collected and concentrated using a SpeedVac. The residues were reconstituted in 100 μL of MeOH/H2O (1:9) and transferred to a 96-well plate for LC-HRMS analysis.

Protocol 2 : Higher concentration metabolites (Trp and 3-IS), were extracted from 10 μL of serum. After addition of the internal standards and 500 μL of MeOH, the samples were vortexed, then homogenized and centrifuged as described above

For 10 mice out of 50, data were missing in the urine. Using all metabolomics data except compartment-metabolites associations for which levels were equal to 0 in all mice, we imputed those missing values using the *mice* function from the ''mice'' package v3.14.0,[110] with arguments m = 10, method = ''pmm'' (predictive mean matching) and seed = 123.

EC enzymes and Metacyc pathways analysis

Microbial gene family abundances in metagenomic DNA reads were estimated using HUMAnN 3.0.[115] Gene families were further mapped to the EC enzymes database and the MetaCyc metabolic pathway database included in HUMAnN3 to obtain the corresponding abundances. Stratification with species contribution was obtained in HUMAnN3 using the KEGG database. Tables of pathway and enzyme abundance obtained were normalized to copies per million (CPM), including unmapped and unintegrated read mass, using the humann_renorm_table function of HuMAnN3.

Statistical analyses

All biostatistical analyses were performed using R v3.6.3. Only microbial SGBs with a minimum prevalence of 30% (i.e., with at least 30% of values strictly above 0, n = 188 SGBs) were considered in all the analyses. Similarly, only EC enzymes or Metacyc pathways with a minimum prevalence of 30% were considered for correlation analysis. Spearman's correlation tests were performed to compute p-values and correlation coefficients. p-values were corrected according to the false discovery rate (FDR), using the Benjamini-Hochberg procedure. These two steps were performed using the *cor.test* and *p.adjust* functions of the ''stats'' package (v3.6.3).[111]

In the GF vs. CV mice analysis, median differences of metabolites abundances between the two types of mice were assessed using Wilcoxon rank-sum test (or Mann-Whitney test), implemented with the *wilcox_test* function of the ''rstatix'' package (v0.7.0).[112]

Guilds' construction

Spearman's correlation coefficients were calculated on relative abundances of each pair of SGBs (function *cor.test* of the ''stats'' package) and a dissimilarity matrix was constructed using the correlation coefficient. This matrix was then subjected to hierarchical clustering following Ward's method (function *hclust* of the ''stats'' package, method = ''ward.D2'')[119] that minimizes the within-cluster variance according to the sum-of-squares criterion. The resulting clustering tree was analyzed from the root node with a procedure to choose the optimal number of clusters. Specifically, at each node, a Permanova test was used to test if the values in the two subtrees were significantly different (using function *adonis* of the ''vegan'' package (v2.5-7)[113]). If the subtrees were indeed statistically different (p-value <0.05), the exploration continued in the two corresponding branches independently, repeating at each new node the same Permanova statistical test. If the two clades were not significantly different, they were considered to form a unique guild, and the exploration was stopped for that branch. In the end, a partition of the SGB pool was formed, with significantly different guilds that do not necessarily correspond to a fixed height in the tree. The guild size ranged from 2 to 11 SGBs. This procedure was implemented by re-factoring the methodology by Wu et al., 2021.[37]